sustainability

MDPI

Article

An Integrated Approach to Map the Impact of Climate Change on the Distributions of *Crataegus azarolus* and *Crataegus monogyna* in Kurdistan Region, Iraq

Kalthum O. Radha and Nabaz R. Khwarahm *

Department of Biology, College of Education, University of Sulaimani, Sulaimani 334, Kurdistan Region, Iraq
* Correspondence: khwarahm21302@alumni.itc.nl

Abstract: The hawthorns *Crataegus azarolus* L. and *Crataegus monogyna* Jacq are two ecologically and medicinally important endemic tree species that occur only in forests of oak in the mountain ranges of the Kurdistan region of Iraq (KRI). These species have been degrading across the mountain ranges at an alarming pace due to climate-related factors (e.g., wildfire events and drought) and anthropogenic drivers. Nevertheless, there is a gap in understanding their distributions today and in the future under a changing climate in Iraq. To address the species' knowledge gap and thus establish a baseline for a future management and conservation strategy, this study used field observation records, species distribution modeling integrated with GIS techniques, and relevant environmental predictors to (i) estimate the species' potential distributions and map their current known distributions across unsurveyed areas; (ii) model the species' possible response under several scenarios for a weather change in the future; (iii) map the species' overlap ranges and the direction of the distributions. Results suggest that under two global climatic models (GCMs), BCC-CSM2-MR and CNRM-CM6-1, the overall habitat expansion magnitude for the two species would be less than the overall habitat reduction magnitude. For *C. azarolus*, the habitat range would contract by 3714.64 km^2 (7.20%) and 3550.47 km^2 (6.89%), whereas it would expand by 2415.90 km^2 (4.68%) and 1627.76 km^2 (3.16%) for the GCMs, respectively. Modeling also demonstrated a similar pattern for *C. monogyna.* The species overlap by 7626.53 km^2 (14.80%) and 7351.45 km2 (14.27%) for the two GCMs. The two species' habitat ranges would contract significantly due to the changing climate. The direction of the species' potential distribution would be mostly toward the KRI's east and southeast mountain forests. Our results, for the first time, provide new data on the species' present and future distributions and outline the advantages of distribution modeling combined with geospatial techniques in areas where species data are limited, such as Iraq.

Keywords: distribution; habitat shift; mountain ecosystem; predictive modeling; vascular plant

check for updates

Citation: Radha, K.O.; Khwarahm, N.R. An Integrated Approach to Map the Impact of Climate Change on the Distributions of *Crataegus azarolus* and *Crataegus monogyna* in Kurdistan Region, Iraq. *Sustainability* **2022**, *14*, 14621. https://doi.org/10.3390/su142114621

Academic Editor: Jasmin Mantilla-Contreras

Received: 27 September 2022
Accepted: 31 October 2022
Published: 7 November 2022

Publisher's Note: MDPI stays neutral with regard to jurisdictional claims in published maps and institutional affiliations.

Copyright: © 2022 by the authors. Licensee MDPI, Basel, Switzerland. This article is an open access article distributed under the terms and conditions of the Creative Commons Attribution (CC BY) license (https://creativecommons.org/licenses/by/4.0/).

1. Introduction

Crataegus L., hawthorn, is a clearly described species member of the tribe Crataegeae and the Rosaceae family [1]. It is constituted of deciduous thorny shrubs and small trees that can grow to a height of up to ten meters [2]. This genus has a wide geographic distribution across temperate Asia, Europe, and North America [3]. It includes around 200–1200 species [4]; from this number, around 50 species are found in the northern hemisphere [5], especially in Turkey and Iran, which contain a large number of species [6], and the mountains of Zagros are approximately home to 17 different species of hawthorn [7]. The Kurdistan region of Iraq (KRI) is restricted to the north, and the northeastern part of Iraq occupies 5% of the country's total area and is part of the Taurus–Zagros mountain range, with altitude ranges between 1000 and 3000 m.a.s.l. [8].

Based on the available investigations, four endemic hawthorn species have been identified in Iraq and the KRI, notably *C. azarolus*, *C. monogyna*, *C. pentagyna*, *and C. meyeri* [6]. Only oak forests in the KRI's mountain ranges are home to these species, which are

frequently combined with other species of plants such as *Quercus aegilops* [9]. Moreover, the most common species among these four in these forests is *C. azarolus* [6]. Hawthorn is extremely valuable for a variety of reasons, including medicinal and ecological benefits [10]. This plant's leaves, flowers, and berries are exceptionally nutrient-dense and have traditionally been used for their medical and health benefits [11].

In addition, these species play a significant ecological and economic role in fields such as biological diversity, human nutrition, wildlife, industrial wood materials, potential energy sources, erosion control, and urban afforestation [12]. However, these species have been degrading across the mountain ranges of the KRI at an alarming pace due to climate-driving factors (e.g., wildfire and aridity) and anthropogenic drivers (e.g., overexploitation, cutting, degradation and shifting in agricultural practices, changes in land cover/land use, lack of forest management strategy, civil war, and political instability) [13–15]. A recent study by analyzing the time-series NDVI (Normalized Difference Vegetation Index) has demonstrated that forests in the KRI suffered fluctuations during the period between 1984 and 2015 [16]. Additionally, between 1990 and 2000, the United Nations Security Council's (UNSC) economic sanctions had a substantial impact on the KRI's woodlands. During this period, people were forced to overexploit the forests, primarily for firewood, because of the poverty and unemployment brought on by the 10-year embargo [9,17]. In the context of climate change, the habitat degradation caused by these factors might become more threatening. Changes in climate have been demonstrated to impact several species' ranges by expanding or contracting them [18]. Providing information on the response of plant communities to future climate conditions aids in better understanding the functions and integrity of the forest ecosystem. Furthermore, forest degradation in the KRI is a critical issue, yet monitoring and managing the degradation has received minimal attention from the government because of the political instability and regional conflict between various sects, predominantly in the country's mountain regions.

In Iraq, at present, studies about hawthorn have only been conducted on the following scopes: for example, their chemical compositions [7,19], taxonomy and anatomy [4,6], and pharmacological activities [20]. Others have investigated the genetic diversity of hawthorn [21] and morphological variety [22]. In Egypt, Moustafa, et al. [23] noted that the *Crataegus sinaica* environment has continuously worsened during the past few years. In Turkey, various studies explored the chemical characteristics of hawthorn fruit [2], molecular characterization [5], and morphology and chemical composition [24]. Moreover, globally, numerous studies have been published on diverse topics such as phylogeny, taxonomy, molecular analysis, and the complete chloroplast genome sequence in some hawthorn species [25–27]. There is still a gap in understanding their geographical distributions and their response to climate change conditions. According to our review, no research has examined these species' spatial dimensions concerning important environmental variables and their potential future statuses under scenarios of climate change in Iraq.

A special platform for mapping present and prospective future distributions is provided by geographic information system (GIS) and species distribution models (SDMs) technology, as well as estimating possible habitat shifts due to changes in climate [28,29]. SDMs evaluate a species' existence and its relevance to other factors at a location, and its environmental and/or spatial characteristics. They are used for a variety of objectives such as biogeography, ecology, and conservation biology [30–32]. The outputs of SDMs are widely utilized to help decision-making authorities in conservation management and planning. The maximum entropy (Maxent) [33], a machine-learning method, is one of the most widely used and approved SDMs; it relies on data from only presence records [34]. By using current distribution data and a variety of environmental variables, the model can simulate and estimate the prospective species' geographic distribution [35].

This study aims to (1) map the current known distribution of *C. azarolus* and *C. monogyna* and forecast the KRI's possible habitat distributions; (2) model and evaluate how the two species' ranges may be impacted by possible future changes in climate; (3) identify the most important environmental parameters for controlling the species' distribution;

(4) map the species' overlapping ranges. For these aims, current climatic conditions, the Maxent model integrated with GIS techniques, and two global climatic models (GCMs) under three shared socioeconomic pathways (SSPs; 126, 245, and 585) for the three time-windows 2041–2060, 2061–2080, and 2081–2100 were used.

2. Materials and Methods

2.1. Study Area

An area of 438,000 km^2 is covered by the Republic of Iraq, which is bordered to the north by Iran and the east by Turkey in the Middle East (at 37°10′ N 47°00′ E), and likewise to the west by the Kingdom of Saudi Arabia and Jordan and to the south by Kuwait. There are four distinct topographic areas in Iraq based on the type of land terrain mountain region (northeast, i.e., KRI), Western Plateau, Jazera, Mesopotamian plain, and Plateau and Hills Regions [8]. Because their ~800 to 3544 m.a.s.l. are considered high heights, the highlands are generally inaccessible and remote [36], with a 35–40 °C temperature range on average. Precipitation is primarily seasonal and varies from 1200 mm in the north to 375 mm in the south (https://gov.krd/english/, accessed on 16 August 2022). Iraq has a short, cold winter and an extremely hot, dry summer due to its subtropical continental location [37].

In Iraq, 4% of the nation's total geographical area comprises natural forests. These forests are almost exclusively located in the KRI, a mountainous region in the country's extreme north and northeast [14]. The KRI (37°38′ N 46°35′ E) has a total size of 51,520.80 km^2 and is made up of three big cities, including the capital city of Erbil, Sulaimani, and Duhok. Considering the currently accessible literature, in Iraq and the KRI, only four unique hawthorn species have been identified [6,38]. Furthermore, they are naturally found in the KRI's forested mountain regions. In this study, we focused only on two species of *Crataegus*, which are *C. monogyna* and *C. azarolus*, due to the two species' important ecological and economic contributions to Iraq. The field data were collected, particularly in the Sulaimani governorate. The KRI governorates (i.e., the highlands) have similar forest structure and composition, climate, and physiography. As a result, this research and modeling is focused on the north of the country, especially the KRI (Figure 1).

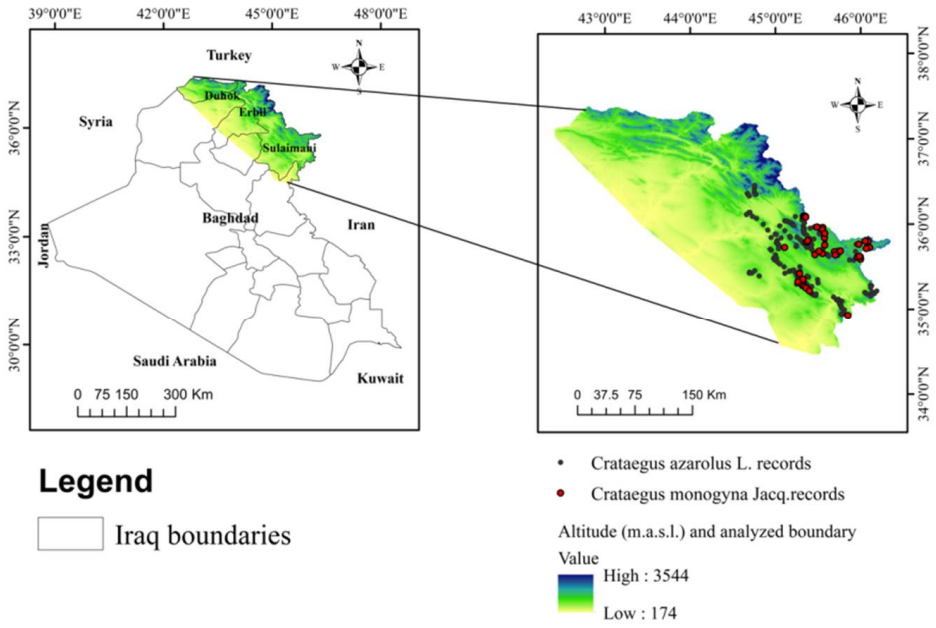


Figure 1. Iraqi governorates borders and the study site, with the occurrence points of *C. azarolus* and *C. monogyna* (The survey area).

2.2. Species Occurrence Data Collection

Several field surveys were conducted to gather the occurrence data points for *C. azarolus* and *C. monogyna* between 2021 and 2022 in Sulaimani governorate by a hand-held device for global positioning system (GPS) (GARMIN-ETREX 22X). These datasets were verified for accuracy (e.g., location correctness utilizing Google Earth and survey) and geographical representativeness [39]. Furthermore, for covering the study area, a stratified random sampling technique was used [40]. These surveys for this study indicated the actual number of the species was 437 points, but the number of points was reduced after removing duplicates and applying spatial filtering to 264 records (n = 227, n = 37, for both species, respectively), which were maintained and utilized. In addition, to decrease spatial autocorrelation between the sites, a spatial filtration of at least 1 km distance was performed on the dataset [41]. Reduced sample bias is an advantage of spatial filtering, which can have a negative impact on distribution models [42]. Additionally, by improving transferability and reducing overfitting of the model, the filtering may produce more reliable model outputs [43]. ArcGIS 10.4.1 was used for quality verification and spatial filtering and extended SDMtoolbox 2.4 [44].

2.3. Environmental Data Sources

Precipitation and temperature were found to be the most critical elements affecting the *Crataegus* genus' habitat suitability [3,45]. In the KRI, the natural habitat for *C. monogyna* and *C. azarolus* is the high-forested mountain ranges, which mainly cover Erbil, Sulaimani, and Duhok (Figure 1). The KRI's spatial extent has been used to select our model boundary, and the environmental variables for our modeling in accordance with this spatial extent were also retrieved [46].

The most prevalent and important factors determining species distribution are identified as the 19 bioclimatic factors (Table A1 in Appendix A) [47,48]. Additional details, including soil supplement and land feature information, are also important [49,50].

Therefore, this research built the model using a combination of climatic, edaphic, and topographic variables, and 26 environmental variables that might influence the geographical distribution of *C. azarolus* and *C. monogyna* were preliminarily selected and listed in (Table A1 in Appendix A). Climatic variables for the "current" 1970–2000s and the future 2041–2060s, 2061–2080s, and 2081–2100s were obtained from the Global Climate Database (WorldClim: http://www.worldclim.org/, accessed on 19 March 2022).

The current climate data has spatial resolutions of 30 s (approximately 1 km^2), and two global climate models (GCMs) have been used to determine the following future climatic scenarios: (1) CNRM-CM6-1 model devolved by the Centre National de Recherché Météorologiques (CNRM) and Cerfacs, France [51,52], and (2) BCC-CSM2-MR model evolved by Beijing Climate Center (BCC), China [53]. Based on previous studies, these two GCMs were selected in this study [54–56]. The distribution's future changes were predicted using this data for the species from 2041 to 2100 using three different shared socioeconomic paths (SSPs): SSP126, SSP245, and SSP585. The SSPs chosen for this study were in three periods: 2041–2060, 2061–2080, and 2081–2100.

The topographic variable, which included a digital elevation model (DEM), slope, and aspect, evolved with the Shuttle Radar Topography Mission (SRTM) (http://srtm.csi.cgiar.org/srtmdata/, accessed on 21 February 2022). The aspect and slope in degrees were calculated using the DEM. In addition, various edaphic elements (soil carbon, soil pH, and soil moisture) were gained via the Center for Sustainability and the Global Environment (SAGE) (http://www.sage.wisc.edu/atlas/index.php, accessed on 17 January 2022). Pearson's correlation analysis ($R^2 \leq 0.8$) was used before modeling to investigate the environmental factors interacting with one another (i.e., collinearity issue) [3,57]. ArcGIS 10.4.1 and the SDMtoolbox were used to conduct Pearson's pairwise correlation analysis for the predictors [58]. Finally, 8 variables were obtained through 26 variables (Table A1 in Appendix A) and were employed in the model's construction because of the variables' significant spatial connection (collinearity) [59].

2.4. Model Building

In this study, the maximum entropy model (Maxent Version 3.4.3) [33] was used to predict the geographic distributions of *C. azarolus* and *C. monogyna* in the KRI in Iraq. Maxent utilizes only presence data with the environmental variables [60]. The algorithm determines the probability distribution of species occurrence while still being constrained by the environment [32,61]. The model is regarded as one of the most effective approaches [42,62].

The KRI's area was used as the model's border (i.e., northeast), in which the species' native habitat is forested mountains (Figure 1). In our models, we selected 70% of the presence data for model training and 30% for model testing while keeping other values as default, as recommended by Phillips et al. [63], resulting in practically decent outputs. Nevertheless, the nature of the input data, the modeler's local knowledge of the study location, and the model's parameterization could all have a substantial impact on the model's output reliability. In other words, the default-mode settings would not always provide reliable models [39,64].

The algorithm's maximum entropy was reached after 500 iterations, and the model replicate selection was set at 10 in this study. The 10 model replicate options also yielded average suitability maps displaying the occurrence probability for *C. azarolus* and *C. monogyna.* Moreover, the background points were set to 525 and 125, respectively, to account for the two species' respective existence records (n = 227, n = 37). The model's regularization multiplier (β) was set to the default value (1). The complexity and simplicity of the model can be affected by changing this value within the model. For instance, lowering the value to less than one makes the model more complicated, while raising it to more than one makes the model simpler [64]. For the purpose of identifying elements when absent and reducing the model's dependability, Jackknife studies were performed [61]. The performance of the developed model is assessed using the area under the receiving operator curve (ROC) value. The area contained by the receiver operator characteristic curves (ROC) in the model is denoted by (AUC) [65,66]. Theoretically, the AUC value varies from 0 to 1, and a score of 1.0 indicates perfect discrimination [67,68].

The Jackknife approach was used to estimate the contribution to the probability of a species' habitat distribution and the variable's relative significance [69]. The logistic output from Maxent "Maximum test presence Logistic threshold" was utilized to create a species grid map showing the probability of their continued existence, with the existing range of presence probability being from 0 to 1. The most effective models were those with the greatest (AUC) values for the two species after 10 iterations. The generated files were converted to a grid pattern using ArcGIS (10.4.1) for further investigation [66].

Finally, Pixel values that are equal to or higher than 0.30 were considered a suitable area for the distributions of both *C. azarolus* and *C. monogyna*. However, pixels with values less than 0.30 were considered as an unsuitable area for the distribution of the species. According to the distribution threshold (i.e., maximum test presence), it can be considered that the distribution maps of *Crataegus* species were classified as following: for C. *azarolus*, unsuitable (0.0–0.30), low suitable (0.30–0.38), medium suitable (0.38–0.59), high suitable (0.59–0.78); and for *C. monogyna*, unsuitable (0.0–0.30), low suitable (0.30–0.41), medium suitable (0.41–0.61), high suitable (0.61–0.81) [37]. These operations were carried out utilizing the ArcGIS 10.4.1 platform's spatial analysis techniques.

2.5. Model Evaluation

A crucial step in model building is evaluating the prediction performance of models. This type of assessment aids in establishing a model's suitability for various uses. It also serves as a foundation for evaluating various modeling methodologies and competing models, as well as identifying the areas of a model that need to be the most improved [70]. For example, to evaluate the discriminating capacity, measurements such as the area under the receiving operating characteristic curve are frequently utilized (i.e., the ability to accurately categorize absences and presences) in SDMs [71]. ROC, or the receiver operating characteristic curve's area under the curve (AUC), is a model accuracy metric that contrasts

accurate and inaccurate predictions over a range of thresholds [72]. The value range for AUC is from 0 to 1, indicating that the model's prediction result is more accurate the closer the AUC value is to 1 [73,74]. A large AUC value indicates a better model performance [72]. The AUC values could be classified as follows: more than 0.9 represents high accuracy, 0.7–0.9 represent acceptable accuracy, and less than 0.7 represents low accuracy [75].

2.6. Current and Future Habitat Distributions Change Analysis for the Species

A range of spatial tools on the ArcGIS platform is utilized to identify change detection between present and future habitat distributions. Habitat suitability maps were used to assess the current and future distributional changes. In the KRI, the distributions were categorized into four classes of potential habitats: (i) expansion of the species' range, or regions that may be suitable for it in the future in 2041–2060, 2061–2080, and 2081–2100; (ii) unsuitable (i.e., regions that would continue to be unsuitable in the future based on the existing environmental conditions); (iii) stable places that the species has previously colonized and will continue to occupy in the future; (iv) a reduction in range (future shrinkage of each species' habitats). Employing a Python-based GIS program known as the SDM toolbox [44], the centroids for present and appropriate prospective regions were compared, as well as the patterns of change in suitable areas. This study's primary goal was to list the major distributional changes of *C. azarolus* and *C. monogyna*. It was accomplished by narrowing the range of these species' geographic distribution to a single-centroid (center) location, and the expected change's magnitude and direction were then represented in a shape file. Furthermore, the areas where the habitat overlap for both species for the (GCMs), BCC-CSM2-MR, and CNRM-CM6-1 were mapped by employing the binary map layers of *C. azarolus* and *C. monogyna* using the raster calculator tool in the ArcGIS platform, and then the pixel numbers of overlapping areas were converted to kilometers for the study area.

3. Results

3.1. The Model's Performance

In this study, according to their AUC > 0.80, all models were excellent to good; the results showed that the model performance for the *C. azarolus* and *C. monogyna* were AUC = 0.80 ± 0.02 and AUC = 0.85 ± 0.05, respectively. These values were close to 1, with the AUC values greater than 0.75; this indicates a great match for the model being used [76]. For the former species, the model showed greater discriminatory power. Moreover, the two models effectively estimated the distribution probability for the two species' habitat suitability under the chosen environmental parameters in the KRI.

3.2. Determinants of C. monogyna and C. azarolus Distributions

The contribution rate of climate factors to the adaptability of *C. azarolus* and *C. monogyna* are shown in Figures A3 and A4 in the Appendix A. The greater the contribution value, the greater the effect of this characteristic on the probability of a species' existence. The climate variable with the largest contribution rate for *C. azarolus* was the annual mean temperature (Bio1 by 57.4%), followed by the seasonality of precipitation (coefficient of variation) (Bio15 by 21.4%) and slope (by 7.2%). The cumulative contribution rate was 86%, showing that these factors had the greatest effect on estimating the probability of *C. azarolus* in the KRI habitat distribution. On the other hand, soil pH and soil carbon demonstrated the lowest contribution (Figure A3 in Appendix A). For *C. monogyna*, the mean value for yearly temperature (Bio1 by 67.9%), diurnal temperature mean value (Bio2 by 19%), and precipitation seasonality (Bio15 by 6%) were collectively contributed by 92.9% to the spatial distribution of the species. However, soil carbon and slope had the least significant proportional contributions to the probability of habitat distribution (Figure A4 in Appendix A).

In response to the target species for the climatic conditions, based on the higher probabilities (from 0.5% onwards), certain factors were shared by both species, including

optimum yearly mean temperature ranges (13–17 °C; 11–16 °C), precipitations per year (920–1030 mm; 970–1000 mm), and precipitation seasonality (83–102 mm; 75–103 mm), respectively. These results imply the importance of water availability and moderate temperature ranges for the distribution of the species in the KRI and Iraq.

Regularizing training gains (%) and AUC variable gains using the Jackknife test in Maxent confirmed that the three climatic variables that had the greatest impact on regularized training were the coefficient of variation of the annual mean temperature (Bio1), annual precipitations (Bio12), and slope; compared to other variables, the distribution of *C. azarolus* is mainly affected by these factors. Furthermore, for *C. monogyna*, the annual mean temperature (bio1), annual precipitation (Bio12), and precipitation seasonally (Bio 15) added additional gains more than other factors in its distribution (Figures A5 and A6 in Appendix A). Finally, the main climatic parameters influencing the potential geographical distribution of *Crataegus* spp. were temperature and rainfall (annual precipitation and seasonal precipitation's coefficient of variation).

3.3. Current and Future Distributions of C. monogyna and C. azarolus

The model findings imply that the existing distribution of *C. azarolus* and *C. monogyna* might be negatively impacted by the changes in climate (Figure 2). In this study, which used two GCMs, the habitat ranges of the two species showed evidence of spatial distributional alteration because of changes in the climate by years (2041–2060, 2061–2080, 2081–2100). For example, for *C. azarolus*, the first GCM model (BCC-CSM2-MR) comparison of the prospective ranges for the future and the present revealed the least difference in 2041–2060 under scenarios SSP126 and SSP245, and the prediction indicated that *C. azarolus* environmental unsuitability regions would rise in trend by 0.50% and 0.70%, respectively. Moreover, with a moderate increase in the unsuitable habitats range in 2041–2060 under scenario SSP585 and in 2061–2080 under scenario SSP126, climate change would increase by 2.75% and 2.58%, respectively. Meanwhile, other scenarios in the years 2061–2080 and 2080–2100 showed a large increase in the unsuitable habitats range (Figure 3; Table 1). In contrast, in the model CNRM-CM6-1 (126, 245, and 585 SSPs), climate change scenarios in 2041–2060, 2061–2080, and 2081–2100 indicated a clear change in the range and increase in the present unsuitable areas by 3.13% under SSP126 in 2041–2060 and 4.50% under SSP585 in 2081–2100 (Figure 4; Table 2).

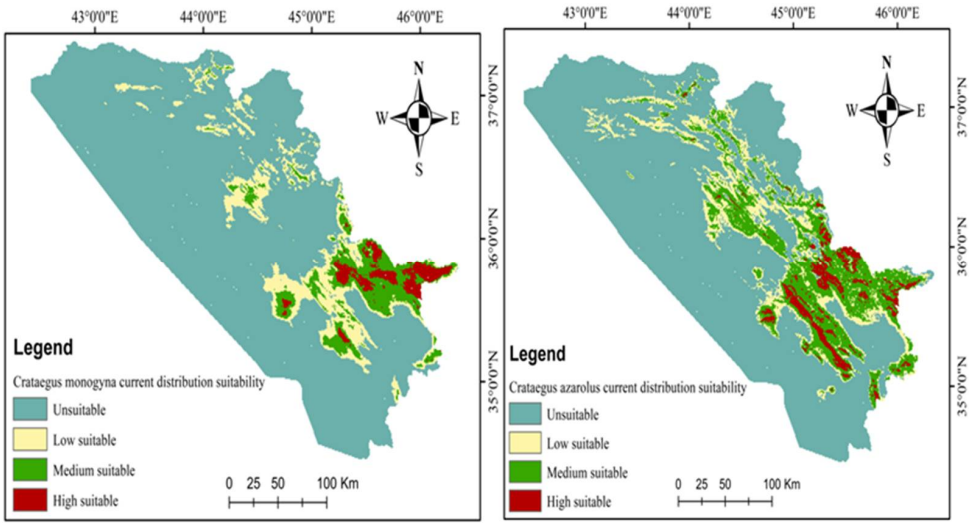


Figure 2. Current habitat distributions of *C. monogyna* and *C. azarolus*.

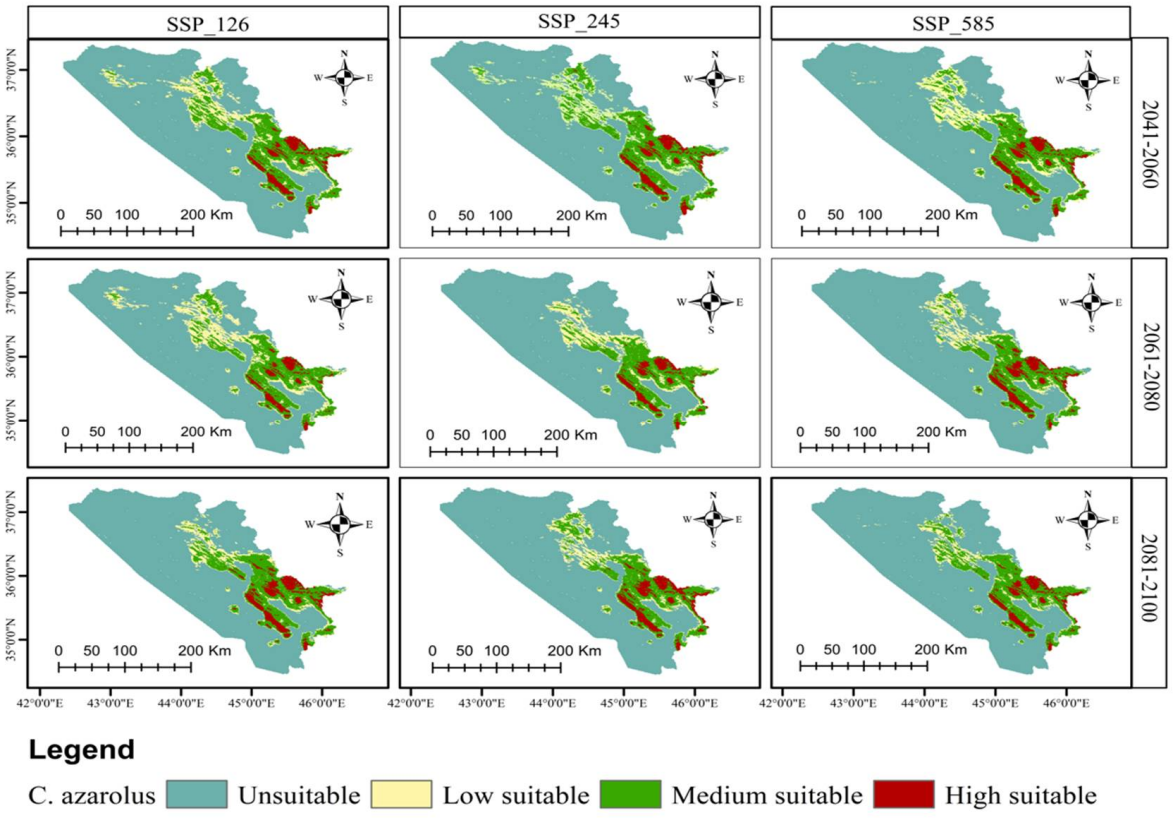


Figure 3. Future habitat distributions of *C. azarolus* in BCC-CSM2-MR model under 126, 245, and 585 SSPs and climate change scenarios in 2041–2060, 2061–2080, and 2081–2100.

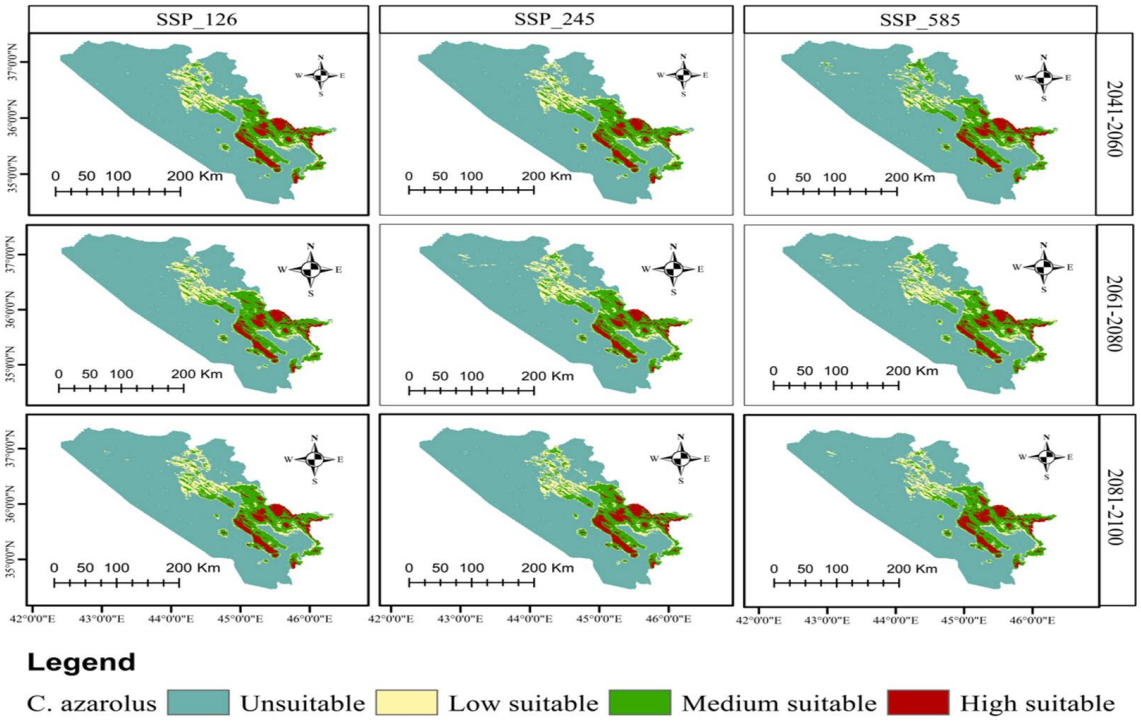


Figure 4. Future habitat distributions of *C. azarolus* in CNRM-CM6-1 model under 126, 245, and 585 SSPs and climate change scenarios in 2041–2060, 2061–2080, and 2081–2100.

Table 1. Modeled regions of habitat appropriateness and unsuitability for the present and future (percentage) of *C. azarolus* in BCC-CSM2-MR model under 126, 245, and 585 SSPs and climate change scenarios in 2041–2060, 2061–2080, and 2081–2100.

		Unsuitable	Low Suitable	Medium Suitable	High Suitable	Increases in Unsuitable Area	Decreases in Total Suitable Area
		Area km^2 (%)	Area km^2 (%)	Area km^2 (%)	Area km^2 (%)	%	%
Current		37,167.90 (72.15)	5331.29 (10.34)	7321.48 (14.22)	1700.13 (3.29)		
2041–2060	SSP126	37,430.21 (72.65)	4700.34 (9.12)	7674.13 (14.89)	1716.12 (3.33)	0.50	−1.83
	SSP245	37,536.70 (72.85)	4691.29 (9.10)	7425.10 (14.41)	1867.71 (3.63)	0.70	−2.57
	SSP585	38,591.20 (74.90)	4336.53 (8.42)	6883.22 (13.36)	1709.85 (3.32)	2.75	−9.92
2061–2080	SSP126	38,500.10 (74.73)	4366.44 (8.48)	6948.06 (13.49)	1706.21 (3.31)	2.58	−9.28
	SSP245	39,158.10 (76.00)	4012.39 (7.79)	6668.37 (12.85)	1721.94 (3.34)	3.85	−13.59
	SSP585	39,179.70 (76.04)	3706.99 (7.20)	6560.45 (12.73)	2073.66 (4.03)	3.89	−14.02
2081–2100	SSP126	39,071.90 (75.84)	2902.84 (5.63)	7159.37 (13.90)	2386.69 (4.63)	3.69	−13.27
	SSP245	39,079.50 (75.85)	3340.43 (6.48)	6758.69 (13.12)	2342.18 (4.55)	3.70	−13.32
	SSP585	39,606.82 (76.87)	2733.14 (5.31)	7305.88 (14.18)	1874.96 (3.64)	4.72	−14.35

Moreover, the total areas of suitable habitat (low, medium, and high) of the KRI from the current 14,352.90 km^2 (27.86%) might seriously reduce with the 126, 245, and 585 SSPs of BCC-CSM2-MR to about 14,090.59 km^2 (−1.83%) under SSP126 in 2041–2060, and to 11,913.98 km^2 (−14.35%) under SSP585 in 2081–2100 (Figure 3; Table 1). Moreover, in the CNRM-CM6-1 model, the suitable areas would decrease from about 12,734.80 km^2 (−11.27%) under SSP585 in 2041–2060 to 12,030.16 km^2 (−16.18%) under SSP585 in 2081–2100 (Figure 4; Table 2).

For medium- and high-suitable categories, in the BCC-CSM2-MR model, a minimal increase was shown in medium-suitable habitat areas under the scenarios SSP126 and SSP245 in 2041–2060 by 0.67% and 0.19%, respectively. In contrast, the habitat range for highly suitable categories would increase under all scenarios in 2041–2100 from 0.02% to 1.34% (Figure 3; Table 1). On the other hand, under the CNRM-CM6-1 model and 126, 245, and 585 SSPs, the medium- and low-suitable areas decreased, and only a slight increase was shown in the high-suitable habitat range during 2021–2100 (Figure 4; Table 2). Each GCM (SSP585) had the greatest influence on the KRI's potential area from 2041 to 2100.

For *C. monogyna*, the prediction of the models demonstrated a similar trend of the habitat; for example, the BCC-CSM2-MR (126, 245, and 585 SSPs) model showed a moderate increase in unsuitable habitats ranging from 1.03% under SSP245 in 2041–2060 to 2.54% under SSP585 in 2081–2100 (Figure 5; Table 3). Moreover, the CNRM-CM6-1 (126, 245, and 585 SSPs) model also showed a moderate increase in the unsuitable habitat areas range from 1.86% under SSP585 in 2041–2060 to 2.50% under SSP126 in 2081–2100 (Figure 6; Table 4).

Table 2. Modeled regions of habitat appropriateness and unsuitability for the present and future (percentage) of *C. azarolus* in CNRM–CM6–1 model under 126, 245, and 585 SSPs and climate change scenarios in 2041–2060, 2061–2080, and 2081–2100.

		Unsuitable	Low Suitable	Medium Suitable	High Suitable	Increases in Unsuitable Area	Decreases in Total Suitable Area
		Area km^2 (%)	Area km^2 (%)	Area km^2 (%)	Area km^2 (%)	%	%
Current		37,167.90 (72.15)	5331.29 (10.34)	7321.48 (14.22)	1700.13 (3.29)		
2041–2060	SSP126	38,786.03 (75.28)	3658.28 (7.10)	6724.61 (13.05)	2351.91 (4.56)	3.13	−11.27
	SSP245	39,127.51 (75.95)	3583.89 (6.96)	6821.99 (13.24)	1987.42 (3.86)	3.80	−13.65
	SSP585	39,285.43 (76.25)	2912.58 (5.65)	6895.04 (13.38)	2427.75 (4.71)	4.10	−14.75
2061–2080	SSP126	39,181.82 (76.05)	3423.17 (6.64)	6712.78 (13.03)	2203.05 (4.28)	3.90	−14.03
	SSP245	39,044.43 (75.78)	3576.05 (6.94)	6967.38 (13.52)	1983.94 (3.85)	3.63	−12.72
	SSP585	39,189.40 (76.07)	3658.36 (7.10)	6657.81 (12.92)	2015.23 (3.91)	3.92	−14.08
2081–2100	SSP126	38,854.80 (75.42)	3631.16 (7.05)	6777.49 (13.16)	2257.32 (4.38)	3.27	−11.75
	SSP245	39,098.18 (75.89)	3301.55 (6.41)	6547.24 (12.70)	2573.83 (4.99)	3.74	−13.45
	SSP585	39,490.64 (76.65)	3375.87 (6.55)	6250.21 (12.13)	2404.08 (4.67)	4.50	−16.18

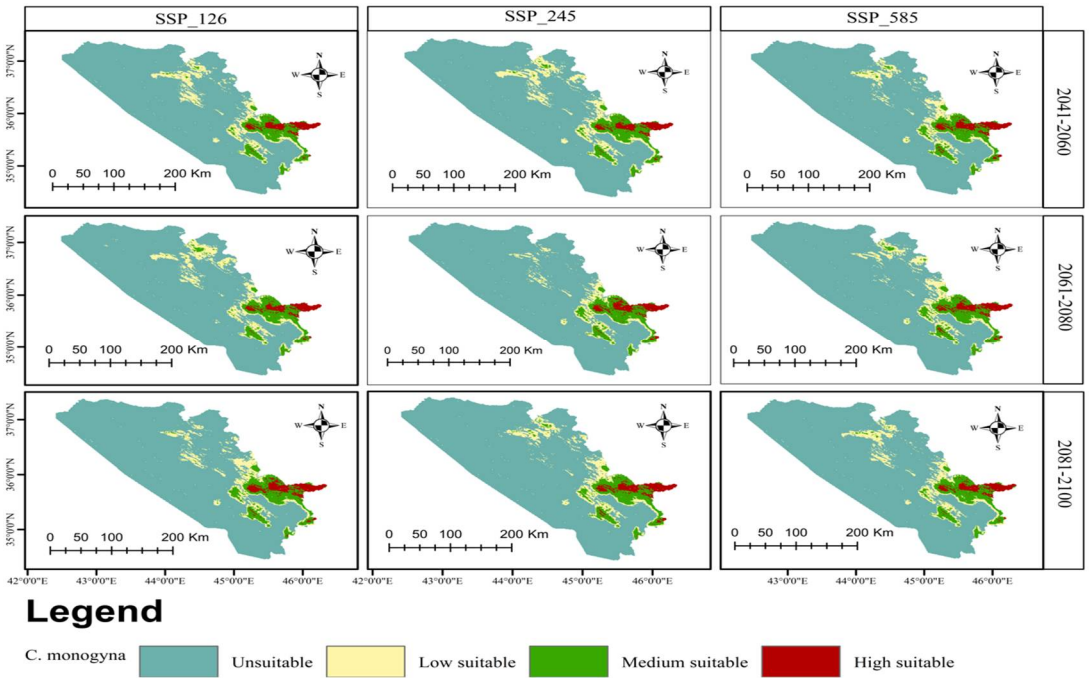


Figure 5. Future habitat distributions of *C. monogyna* in BCC-CSM2-MR model under 126, 245, and 585 SSPs and climate change scenarios in 2041–2060, 2061–2080, and 2081–2100.

Table 3. Modeled regions of habitat appropriateness and unsuitability for the present and future (percentage) of *C. monogyna* in BCC-CSM2-MR model under 126, 245, and 585 SSPs and climate change scenarios in 2041–2060, 2061–2080, and 2081–2100.

		Unsuitable	Low Suitable	Medium Suitable	High Suitable	Increases in Unsuitable Area	Decreases in Total Suitable Area
		Area km^2 (%)	Area km^2 (%)	Area km^2 (%)	Area km^2 (%)	%	%
Current		42,111.70 (81.74)	4979.28 (9.66)	3185.96 (6.18)	1243.78 (2.41)		
2041–2060	SSP126	43,105.80 (83.67)	4129.23 (8.01)	3198.81 (6.21)	1086.96 (2.14)	1.93	−10.56
	SSP245	42,646.02 (82.77)	4485.39 (8.70)	3325.78 (6.46)	1063.61 (2.06)	1.03	−5.68
	SSP585	43,131.53 (83.71)	3735.34 (7.31)	3451.02 (6.65)	1202.91 (2.33)	1.97	−10.84
2061–2080	SSP126	42,822.02 (83.12)	4310.09 (8.37)	3282.65 (6.37)	1106.04 (2.15)	1.38	−7.55
	SSP245	43,181.94 (83.82)	3774.52 (7.05)	3341.09 (6.49)	1223.25 (2.37)	2.08	−11.37
	SSP585	43,021.21 (83.50)	3666.99 (7.12)	3614.47 (7.02)	1218.13 (2.36)	1.76	−9.67
2081–2100	SSP126	43,297.82 (84.04)	3444.04 (6.68)	3583.39 (6.96)	1195.55 (2.32)	2.30	−12.61
	SSP245	43,183.04 (83.82)	3665.25 (7.11)	3562.13 (6.91)	1110.38 (2.16)	2.08	−11.39
	SSP585	43,423.03 (84.28)	3755.68 (7.29)	3219.35 (6.25)	1122.74 (2.18)	2.54	−13.94

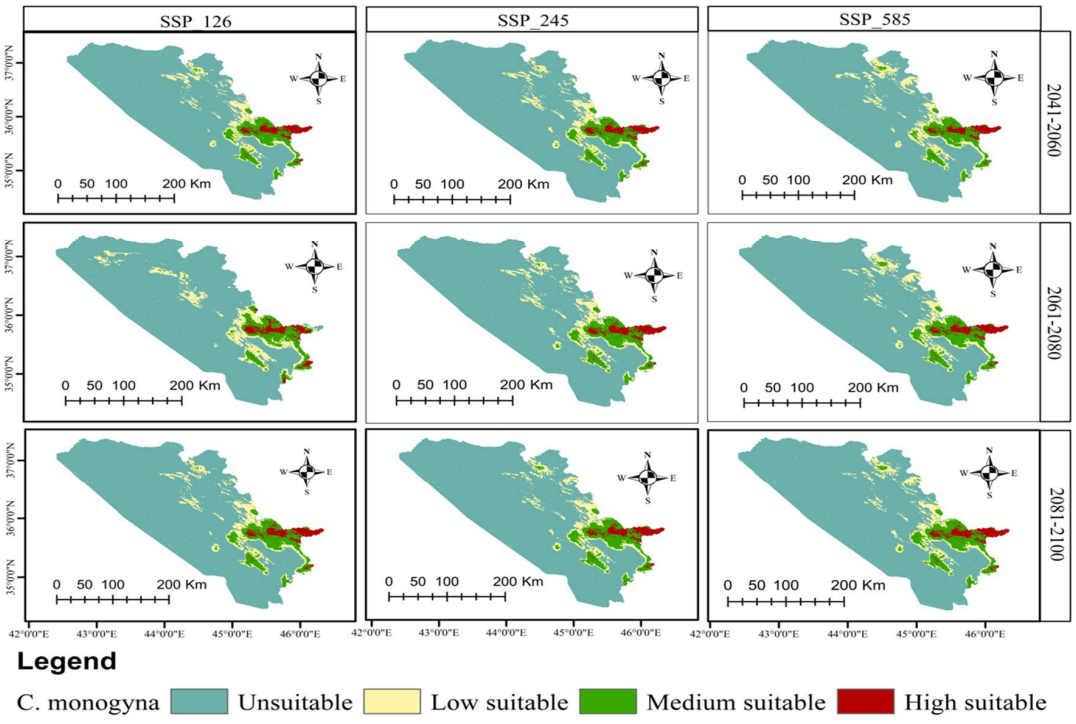


Figure 6. Future habitat distributions of *C. monogyna* in CNRM-CM6-1 model under 126, 245, and 585 SSPs and climate change scenarios in 2041–2060, 2061–2080, and 2081–2100.

Table 4. Modeled regions of habitat appropriateness and unsuitability for the present and future (percentage) of *C. monogyna* in the CNRM-CM6-1 model under 126, 245, and 585 SSPs and climate change scenarios in 2041–2060, 2061–2080, and 2081–2100.

		Unsuitable	Low Suitable	Medium Suitable	High Suitable	Increases in Unsuitable Area	Decrease in Suitable Area
		Area km^2 (%)	Area km^2 (%)	Area km^2 (%)	Area km^2 (%)	%	%
Current		42,111.70 (81.74)	4979.28 (9.66)	3185.96 (6.18)	1243.78 (2.41)		
2041–2060	SSP126	43,262.31 (83.97)	3592.90 (6.97)	3451.69 (6.69)	1213.87 (2.37)	2.23	−12.23
	SSP245	43,267.92 (83.98)	3716.72 (7.21)	3370.30 (6.54)	1165.87 (2.26)	2.24	−12.29
	SSP585	43,068.94 (83.60)	4095.14 (7.94)	3318.83 (6.44)	1037.87 (2.02)	1.86	−10.17
2061–2080	SSP126	43,217.43 (83.88)	3826.00 (7.43)	3346.31 (6.50)	1131.09 (2.19)	2.14	−11.75
	SSP245	43,314.50 (84.07)	3640.90 (7.07)	3372.39 (6.55)	1193.01 (2.31)	2.33	−12.78
	SSP585	43,164.95 (83.79)	3642.29 (7.07)	3556.73 (6.90)	1156.83 (2.24)	2.05	−11.19
2081–2100	SSP126	43,403.55 (84.24)	3536.56 (6.86)	3409.26 (6.62)	1171.43 (2.28)	2.50	−13.73
	SSP245	43,228.93 (83.91)	3531.69 (6.85)	3558.84 (6.91)	1201.34 (2.33)	2.17	−11.87
	SSP585	43,160.06 (83.77)	3546.30 (6.88)	3590.14 (6.97)	1224.30 (2.38)	2.03	−11.14

However, the total area of suitable habitats that are appropriate from the current 9409.02 km^2 (18.26%) would drastically reduce under the 126, 245, and 585 SSPs BCC-CSM2-MR model, from about 8874.78 km^2 (−5.68%) under SSP245 in 2041–2060 to 8097.775 km^2 (−13.94%) under SSP585 in 2081–2100 (Figure 5; Table 3). Meanwhile, in CNRM-CM6-1, the model showed that the decrease in areas of suitable habitat ranges would be from 8451.84 km^2 (−10.17%) under SSP585 in 2041–2060 to 8117.25 km^2 (−13.73%) under SSP126 in 2081–2100 (Figure 6; Table 4). Under 126, 245, and 585 SSPs, the BCC-CSM2-MR and CNRM-CM6-1 models showed a small difference comparing the *C. azarolus* with *C. monogyna*, indicating that in *C. monogyna*, under all scenarios the medium suitable habitat areas would increase from 0.26% to 0.79%. Furthermore, the appropriateness of both the low- and high-suitable area were decreased, and the total areas of the sum of the low-suitable area and high-suitable area would decrease from −1.31% to −3.70% during 2041–2100 (Tables 3 and 4).

3.4. Distribution Change Analysis between Current and Future Habitat for C. azarolus and C. monogyna

Model findings showed that changes in the climate would have a significant effect on the potential distribution of *C. azarolus* and *C. monogyna* in 2041–2060, 2061–2080, and 2081–2100. For example, the GCM, BCC-CSM2-MR, and three shared socioeconomic pathways (SSPs) with 126, 245, and 585 scenarios indicated that the C. *azarolus* habitats range would contract from 2680.94 km^2 (5.20%) under SSP126 in 2041–2060 to 3714.64 km^2 (7.20%) under SSP585 in 2081–2100. In contrast, the habitat would expand from 1274.38 km^2 (2.47%) under SSP585 in 2081–2100 to 2415.90 km^2 (4.68%) under SSP126 in 2041–2060 (Figure 7; Table 5). Moreover, the net loss (contraction) of habitat to the change in climate

for C. *azarolus* would change from −0.52% under SSP126 in 2041–2060 to −4.73% under SSP585 in 2081–2100 (Figure 8; Table 5).

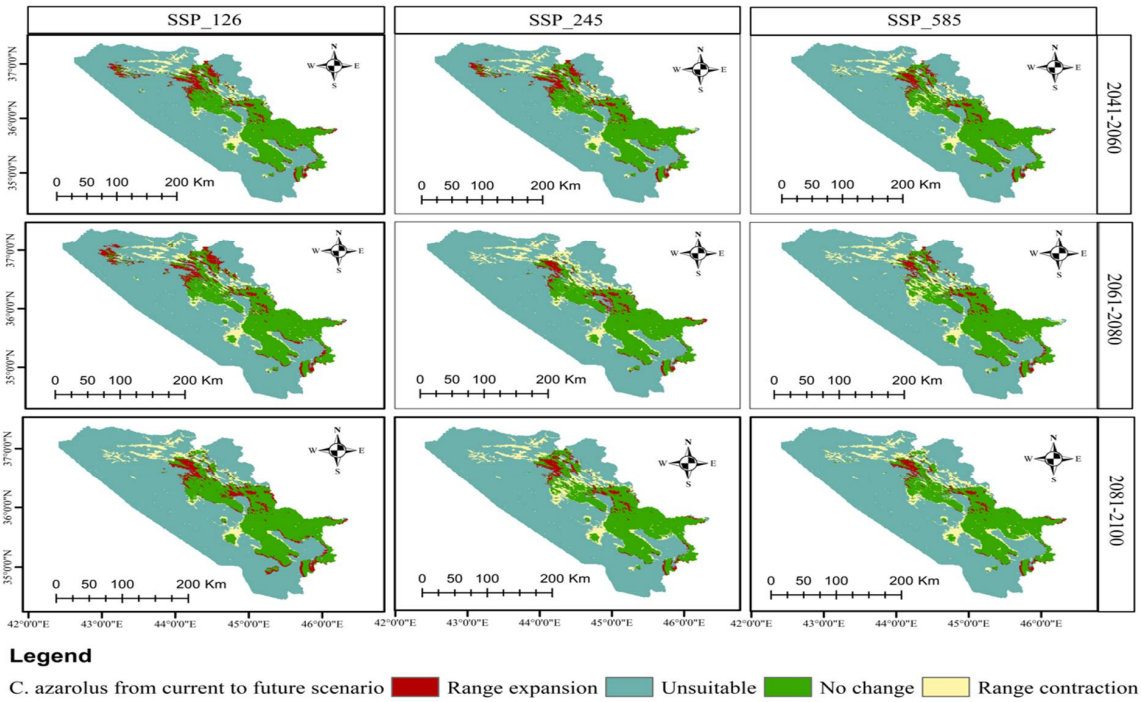


Figure 7. Range shifts in environment distribution between the present and the future of *C. azarolus* in BCC-CSM2-MR model under 126, 245, and 585 SSPs and climate change scenarios in 2041–2060, 2061–2080, and 2081–2100 in the KRI.

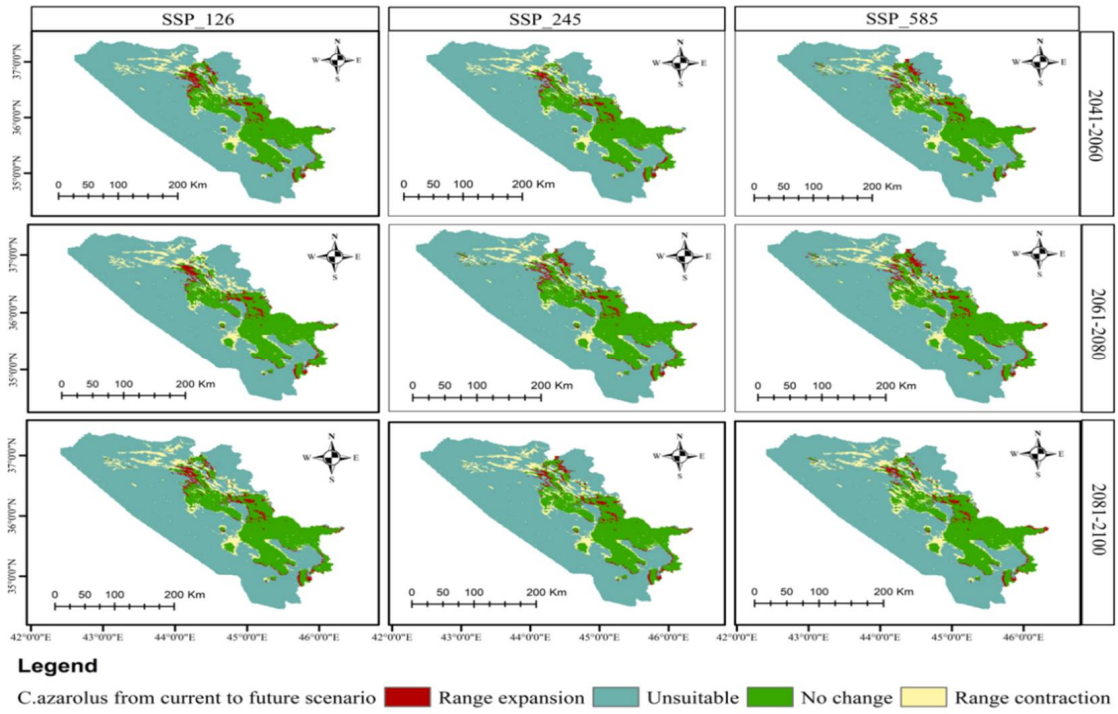


Figure 8. Range shifts in environment distribution between the present and the future of *C. azarolus* in the CNRM-CM6-1 model under 126, 245, and 585 SSPs and climate change scenarios in 2041–2060, 2061–2080, and 2081–2100 in the KRI.

Table 5. Changes in the area of *C. azarolus* suitable habitats (in km^2) under various climatic scenarios in comparison to its existing distribution and the BCC-CSM2-MR model during 2041–2100 in the KRI.

Year	Scenario	Remained Unsuitable	No Change	Range Contraction	Range Expansion	Habitat Change
		Area km^2	Area km^2	Area km^2 (%)	Area km^2 (%)	%
2041–2060	SSP126	34,749.19	11,674.70	2680.94 (5.20)	2415.90 (4.68)	−0.52
	SSP245	34,809.80	11,628.80	2726.85 (5.29)	2355.38 (4.57)	−0.72
	SSP585	35,435.80	11,200.30	3155.35 (6.12)	1729.31 (3.35)	−2.77
2061–2080	SSP126	34,777.82	11,612.79	2742.85 (5.32)	2387.34 (4.63)	−0.69
	SSP245	35,619.50	10,817.00	3538.64 (6.86)	1545.68 (3.00)	−3.86
	SSP585	35,611.10	10,787.10	3568.56 (6.92)	1554.03 (3.01)	−3.91
2081–2100	SSP126	34,955.20	11,742.21	2613.46 (5.07)	2210.00 (4.28)	−0.79
	SSP245	35,589.60	10,867.10	3488.56 (6.77)	1575.58 (3.05)	−3.72
	SSP585	35,890.80	10,641.00	3714.64 (7.20)	1274.38 (2.47)	−4.73

Furthermore, the GCM (CNRM-CM6-1) model showe, the habitat range would contract from 3149.09 km^2 (6.12%) under SSP126 in 2041–2060 to 3550.46 km^2 (6.89%) under SSP585 in 2081–2100, and it would expand from 1225.00 km^2 (2.37%) under SSP585 in 2081–2100 to 1627.76 km^2 (3.16%) under SSP585 in 2061–2080 (Figure 8; Table 6). Thus, the habitat net loss would vary from −3.06% under SSP585 in 2061–2080 to −4.52% under SSP585 in 2081–2100 (Figure 8; Table 6).

For, *C. monogyna*, the BCC-CSM2-MR model also demonstrated the habitat range would contract from 2910.75 km^2 (5.64%) under SSP126 in 2041–2060 to 3293.78 km^2 (6.39%) under SSP126 in 2061–2080. In contrast, the habitat would expand from 1749.50 km^2 (3.39%) under SSP245 in 2061–2080 to 2526.51 km^2 (4.90%) under SSP245 in 2041–2061 (Figure 9; Table 7). Changes in climate would result in a range of habitat losses, including from −1.04% under SSP245 in 2041–2060 to −2.54% under SSP585 in 2081–2100 (Figure 9; Table 7).

Furthermore, for the GCM, in the CNRM-CM6-1 model the habitats range would contract from 2985.63 km^2 (5.79%) under SSP245 in 2061–2080 to 3310.48 km^2 (6.42%) under SSP126 in 2061–2080 (Figure 10; Table 8). However, the habitats range would expand from 1784.28 km^2 (3.46%) under SSP126 in 2061–2080 to 2168.96 km^2 (4.21%) under SSP585 in 2041–2060, and the habitat loss would vary from −1.85% under SSP585 in 2041–2060 to (−2.51%) under SSP126 in 2081–2100 (Figure 10; Table 8).

Table 6. Changes in the area of *C. azarolus* suitable habitats (in km^2) under various climatic scenarios in comparison to its existing distribution and the CNRM-CM6-1 model during 2041–2100 in the KRI.

Year	Scenario	Remained Unsuitable	No Change	Range Contraction	Range Expansion	Habitat Change
		Area km^2	Area km^2	Area km^2 (%)	Area km^2 (%)	%
2041–2060	SSP126	35,635.50	11,206.50	3149.09 (6.12)	1529.68 (2.96)	−3.16
	SSP245	35,830.89	11,059.00	3296.57 (6.41)	1334.21 (2.59)	−3.82
	SSP585	35,786.40	10,858.04	3497.62 (6.78)	1378.74 (2.67)	−4.11
2061–2080	SSP126	35,819.10	10,994.40	3361.27 (6.53)	1346.03 (2.61)	−3.92
	SSP245	35,600.72	11,165.12	3190.49 (6.19)	1564.47 (3.04)	−3.15
	SSP585	35,537.39	11,153.59	3201.95 (6.22)	1627.76 (3.16)	−3.06
2081–2100	SSP126	35,720.34	11,182.52	3173.09 (6.16)	1444.85 (2.80)	−3.36
	SSP245	35,764.19	11,123.00	3232.57 (6.27)	1400.98 (2.72)	−3.55
	SSP585	35,940.19	10,805.09	3550.46 (6.89)	1225.00 (2.37)	−4.52

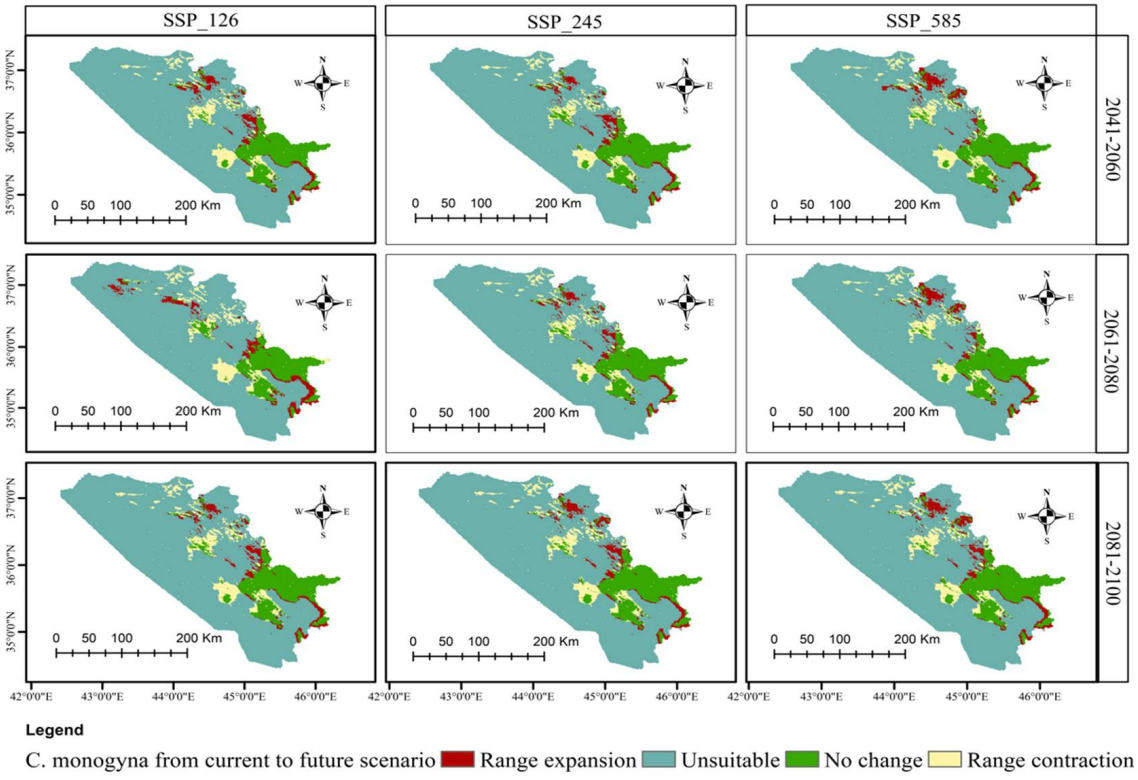


Figure 9. Range shifts in environment distribution between the present and the future of *C. monogyna* in BCC-CSM2-MR model under 126, 245, and 585 SSPs and climate change scenarios in 2041–2060, 2061–2080, and 2081–2100 in the KRI.

Table 7. Changes in the area of *C. monogyna* suitable habitats (in km^2) under various climatic scenarios in comparison to its existing distribution and the BCC-CSM2-MR model during 2041–2100 in the KRI.

Year	Scenario	Remained Unsuitable	No Change	Range Contraction	Range Expansion	Habitat Change
		Area km^2	Area km^2	Area km^2 (%)	Area km^2 (%)	(%)
2041–2060	SSP126	40,045.09	6498.27	2910.75 (5.64)	2066.69 (4.01)	−1.63
	SSP245	39,585.20	6348.27	3060.75 (5.94)	2526.51 (4.90)	−1.04
	SSP585	40,005.40	6284.28	3124.75 (6.06)	2106.35 (4.08)	−1.98
2061–2080	SSP126	39,526.80	6215.24	3293.78 (6.39)	2484.93 (4.82)	−1.57
	SSP245	40,362.23	6484.62	2924.41 (5.67)	1749.50 (3.39)	−2.28
	SSP585	39,772.40	6170.19	3238.83 (6.28)	2339.39 (4.54)	−1.74
2081–2100	SSP126	40,277.40	6391.40	3017.62 (5.85)	1834.36 (3.56)	−2.29
	SSP245	39,903.80	6131.93	3277.09 (6.36)	2207.91 (4.28)	−2.08
	SSP585	40,251.60	6239.06	3169.95 (6.15)	1860.10 (3.61)	−2.54

Table 8. Changes in the area of *C. monogyna* suitable habitats (in km^2) under various climatic scenarios in comparison to its existing distribution and the CNRM-CM6-1 model during 2041–2100 in the KRI.

Year	Scenario	Remained Unsuitable	No Change	Range Contraction	Range Expansion	Habitat Change
		Area km^2	Area km^2	Area km^2 (%)	Area km^2 %	%
2041–2060	SSP126	40,117.40	6264.12	3144.92 (6.10)	1994.36 (3.87)	−2.23
	SSP245	40,250.30	6391.39	3017.62 (5.85)	1861.49 (3.61)	−2.24
	SSP585	39,942.81	6282.88	3126.15 (6.06)	2168.96 (4.21)	−1.85
2061–2080	SSP126	39,942.13	6171.54	3310.48 (6.42)	2096.65 (4.20)	−2.22
	SSP245	40,327.50	6423.39	2985.63 (5.79)	1784.28 (3.46)	−2.33
	SSP585	40,043.00	6288.45	3120.57 (6.05)	2068.79 (4.01)	−2.04
2081–2100	SSP126	40,317.69	6323.23	3085.79 (5.98)	1794.02 (3.47)	−2.51
	SSP245	40,151.50	6331.58	3077.44 (5.97)	1960.27 (3.80)	−2.17
	SSP585	40,074.90	6325.32	3083.71 (6.02)	2036.79 (3.95)	−2.07

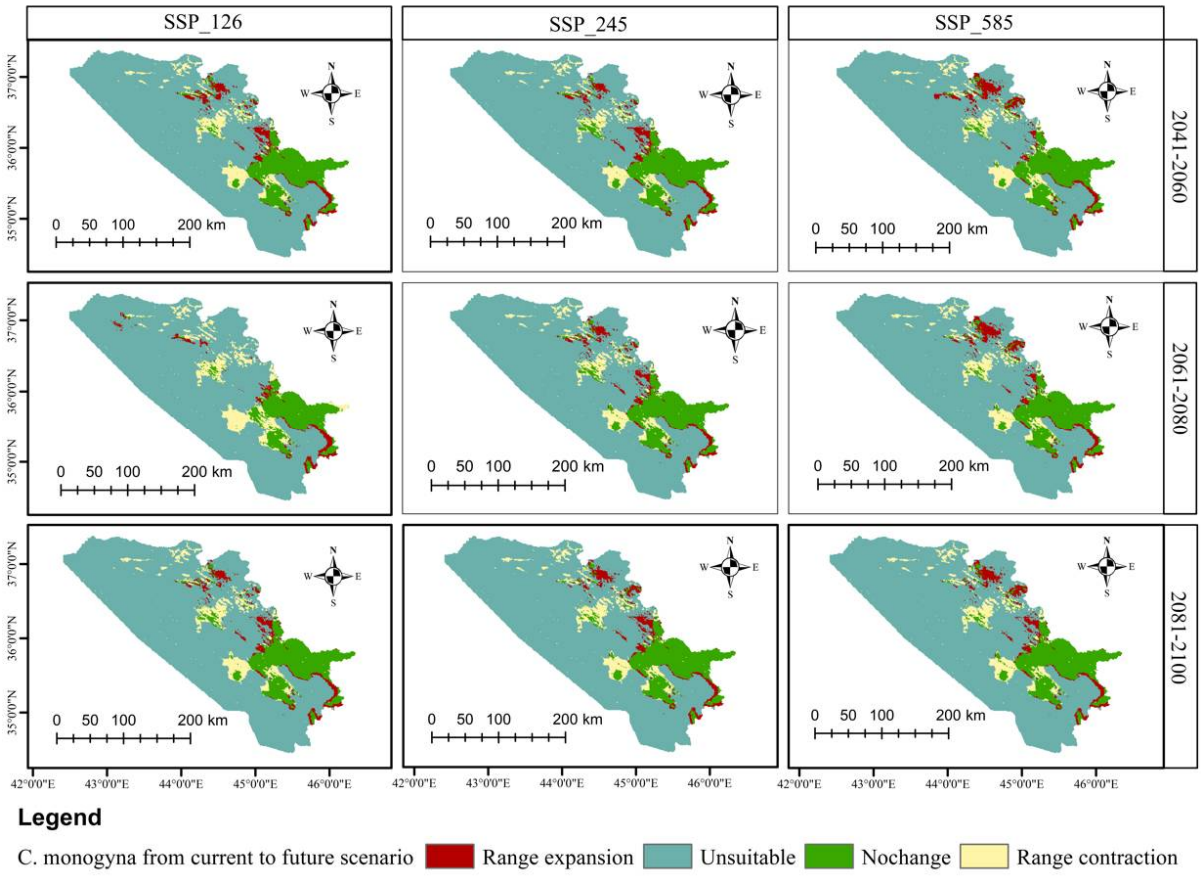


Figure 10. Range shifts in environment distribution between the present and the future of *C. monogyna* in the CNRM–CM6–1 model under 126, 245, and 585 SSPs and climate change scenarios in 2041–2060, 2061–2080, and 2081–2100 in the KRI.

The findings predict that for *C. azarolus*, the scenario SSP585 in 2081–2100 of BCC-CSM2-MR shows a net loss of habitats of −4.73%, and SSP585 in 2081–2100 of CNRM-CM6-1 shows a net loss of 4.52% (Tables 5 and 6). Moreover, for *C. monogyna,* the scenario SSP585 in 2081–2100 of BCC-CSM2-MR shows a net loss of habitat of −2.54%, and the scenario SSP126 in 2081–2100 of CNRM-CM6-1 shows a loss of 2.51% (Tables 7 and 8), which will most likely have a greater impact on the distribution in the future for the two species. Finally, the model discovered that the results of the BCC-CSM2-MR model expectations were fairly identical to the predictions of CNRM-CM6-1, and the variations between GCMs in Maxent were smaller.

3.5. Distributional Change Direction and Migration of Geographical Patterns for C. azarolus and C. monogyna under Future Changes in Climate

The habitat distributional change centroid for *C. azarolus* and *C. monogyna* has projected a clear change in the centroid of the most likely habitats to the southeast parts of the KRI, respectively, under the GCMs, BCC-CSM2-MR and CNRM-CM6-1 models, and three SSP, with 126, 245, and 585 climate change scenarios. In addition, the centroids of the current and future climatic distribution regions were estimated to further explore patterns by using the ArcGIS and SDM toolbox [58].

SDMtools have been used to analysis also by using ASCII data generated under various emission scenarios predicted by the Maxent model, plotting the spatial pattern and centroid changes of the appropriate habitat area of *C. azarolus* and *C. monogyna*. Therefore, to investigate the variations under the current and future scenarios for changes in climate, centroid position changes have been used to represent the change of direction of the total and high-suitability areas and to evaluate the migration distance of the species' useful

plant communities area on longitude and latitude coordinates. Under the majority of the scenarios, with changes in direction and magnitude, the difference between the old and new distribution centroid was slightly stronger. For example, the geographical centroid of the total suitable habitat for *C. azarolus* and *C. monogyna*, under the current climate scenario, was located at the positions 44°59′51.961″ E, 35°57′40.728″ N and 45°9′47.179″ E, 35°51′47.232″ N, respectively. The result of the BCC-CSM2-MR global climatic model showed that the centroids for *C. azarolus* migrated southeastward by about 1.831 km^2 to the new position of 45°1′3.205″ E; 35°57′51.045″ N in 2041–2060 under SSP254, and then shifted about 19.790 km^2 to 45°9′51.472″ E; 35°50′43.428″ N in 2061–2080 under the SSP245 scenario (Figure A1 in Appendix A). Moreover, for *C. monogyna*, the centroid migrated about 7.668 km^2 to the new position of 45°14′37.766″ E, 35°53′4.396″ N in 2041–2060 under SSP254, and then shifted about 22.375 km^2 to 45°22′7.772″ E, 35°44′33.854″ N in 2061–2080 under the SSP245 scenario (Figure A1 in Appendix A).

Although the result of the CNRM-CM6-1 model predicted that most of the centroid directions have the same pattern, which is toward the southeast of KRI, the direction of the centroid for *C. azarolus* migrated southeastward by about 14.521 km^2 to the new position of 45°8′3.036″ E, 35°53′31.755″ N in 2041–2060 under SSP126, and then changed nearly 20.763 km^2 to 45°10′3.52.059″ E, 35°50′54.790″ N in 2081–2100 under the SSP585 scenario (Figure A2 in Appendix A). Furthermore, for *C. monogyna*, the centroid migrated about 14.569 km^2 to the new position of 45°19′38.243″ E, 35°48′46.027″ N in 2041–2060 under SSP585, and then changed to 22.346 km^2 to 45°22′29.874″ E, 35°45′33.474″ N in 2081–2100 under the SSP126 scenario (Figure A2 in Appendix A). The habitat distributional change centroid indicated overlapping habitat areas for *C. azarolus* and *C. monogyna* in the southeast of the KRI, which is an effective way to start and improve conservation strategies and efforts. As a result of the findings, it was determined that *Crataegus* spp. was anticipated to move to higher elevations, which was extremely consistent with the findings of an earlier study [3].

4. Discussion

4.1. Distribution of C. azarolus and C. monogyna Undercurrent and Future Climate Conditions

One of the most significant causes contributing to the fragmentation and loss of ecosystems and declining biodiversity is due to climate change [77–79]. As such, various tools for modeling have been developed to better understand the consequences of climate change on the distribution of plant communities across different ecosystems and ecoregions. The Maxent modeling in this study showed that under all the SSPs scenarios for the two GCMs, BCC-CSM2-MR and CNRM-CM6-1, the habitat distribution ranges for the two species would reduce from their current statuses suggesting there would also be some range expansions for the species. Nevertheless, it follows that the expansion would be smaller than the magnitude of the contraction. In this study, the current and future potential distributions of the two species are mainly controlled by the annual mean temperature (13–17 °C; 11–16 °C) and annual precipitation (920–1030 mm; 970–1000 mm), as demonstrated by the modeling. These optimal ranges slightly vary for the two species; however, the species coexist across a wide range of areas in the KRI (Figures 11 and 12). In arid and semiarid regions, such as in Iraq and the KRI, precipitation plays a key role in the growth and development of plant communities [9]. Springtime plant activity depends on seasonal precipitation, and in arid ecosystems, there may be a direct correlation between the frequency and intensity of precipitation and vegetation productivity [80]. High altitude and this quantity of precipitation are typically associated in the KRI [9]. These results are consistent with earlier researches, which indicated that the oak forest distribution in the nation's northeast is constrained by rain [14,81]. Furthermore, these results are consistent with other studies indicating that precipitation seasonally, annual precipitation, and annual mean temperature are some of the most important factors that influence the different plant species' regional distribution [82,83].

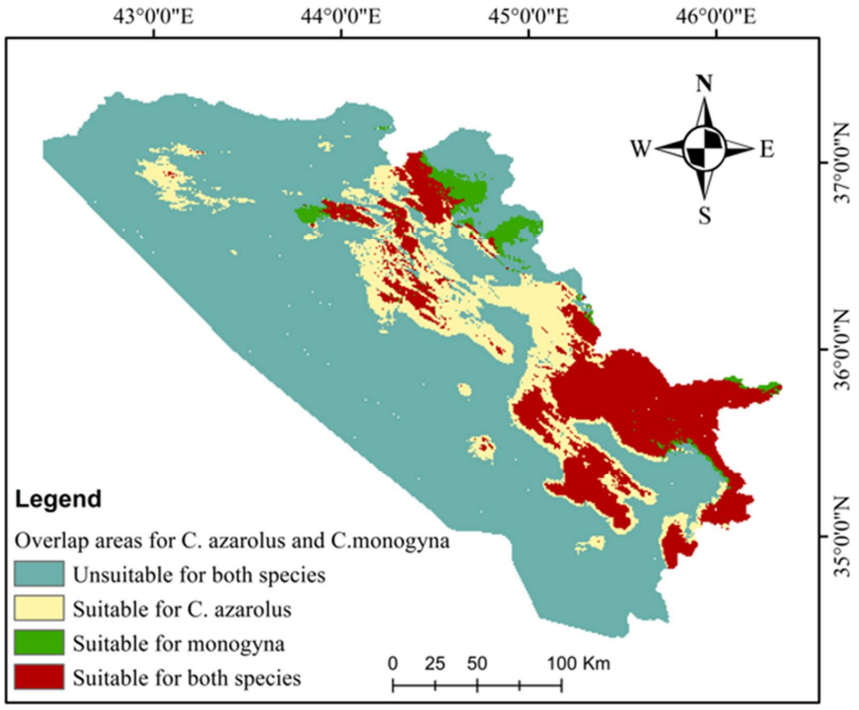


Figure 11. Illustration of overlapping habitat via spatial representation for *C. azarolus* and *C. monogyna* under GCM (BCC-CSM2-MR) model in the KRI.

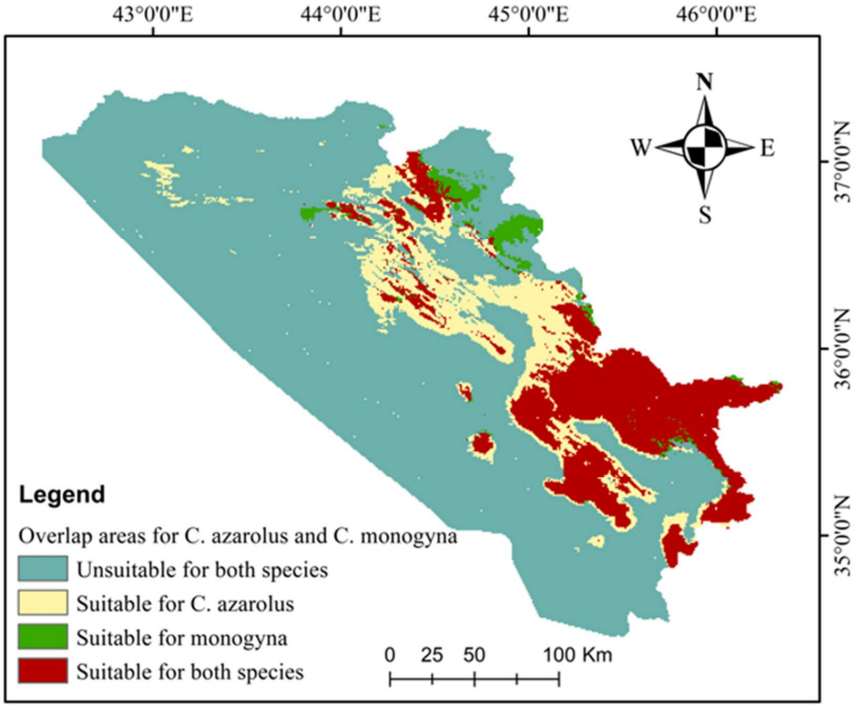


Figure 12. Illustration of overlapping habitat via spatial representation for *C. azarolus* and *C. monogyna* under GCM (CNRM-CM6-1) model in the KRI.

Our results indicate that under the climate change scenarios, the temperature will increase in the KRI and throughout Iraq while precipitation will decrease spatially (possibly resulting in drought). Intuitively, this suggests the contraction of the habitat distribution of the target species in the KRI.

Temperature is also considered an important factor influencing plant development and distribution. The most fundamental metabolic processes in plants are strongly influenced by temperature [84]. In arid and semiarid ecosystems, water availability and air temperature are key main deriving forces in determining plant growth, development, and survival of vegetation [85–87]. In this context, plant phenology in Iraq and the KRI (i.e., arid and semiarid, respectively) is mostly influenced by precipitation, which is considered a crucial climatic condition affecting the distribution of vegetation by pattern and dynamism [80]. The KRI is essentially a mountainous region, with elevations between 174 and 3544 m.a.s.l., and oak forests predominately cover the mountains [14], with a variety of high peaks and valleys that receive significantly more precipitation than the lowlands receive. Therefore, as the climate changes, the extent of the forested and vegetated areas will also change due to the spatial variance of precipitation. These results are in line with findings from previous research that predicted that forest ecosystems would spatially move toward high altitudes when the temperature changed in the northern hemisphere [88–90]. For example, in the Kurdistan Region of Iraq and the Central Zagros [8], it is indicated that scenarios for future changes in climate would result in the *Q. aegilops* distribution ranges being reduced and the centroid of the distribution shifting toward higher altitudes. Moreover, Naghipour, Asl, Ashrafzadeh, and Haidarian [3] noted that the suitable habitat of *C. azarolus* in the future would decline due to climate change scenarios.

4.2. Environmental Variables Controlling the Distribution of C. monogyna and C. azarolus

The primary environmental parameters that affect the distribution of *C. monogyna* and *C. azarolus* were discovered in this investigation by Pearson correlation analysis and the Jackknife cutting method. Based on the results, among the environmental variables, temperature and precipitation primarily contributed as factors in the distribution model for the two species, implying that these variables influenced how they were distributed. The fact that local climatic factors play a crucial role in population renewal confirmed this conclusion [91,92].

Significant environmental elements were shared by both species, including optimum yearly mean temperature ranges (13–17 °C; 11–16 °C), precipitations per year (920–1030 mm; 970–1000 mm), and precipitation seasonality (83–102 mm; 75–103 mm), respectively. Our results, consistent with other studies, indicate that precipitation seasonally, annual precipitation, and annual mean temperature are some of the most important factors that influence the different plant species' regional distribution [9,82]. Furthermore, water availability affects a plant's capacity for photosynthesis; hence, greater availability of water can enhance carbon uptake and increase plant productivity [93,94]. Furthermore, the evapotranspiration brought on by high temperatures and solar radiation is typically not matched by low precipitation levels, which results in arid lands having low overall productivity [95].

According to the model result, *C. azarolus* and *C. monogyna* occur in all habitat types that have a seasonal precipitation range of 83–102 mm and 75–103 mm, respectively. Springtime plant activity depends on seasonal precipitation, and in dryland ecosystems, there may be a direct correlation between the frequency and intensity of rainfall and vegetation productivity [87]. High altitude and this quantity of precipitation are typically associated in the KRI; according to these results, which are consistent with earlier research, it is indicated that the oak forest distribution in the nation's northeast may be constrained by rain [9,14,81]. Furthermore, less annual precipitation, which is predicted by climate change models, as well as more extreme occurrences (the number of rainy days is decreasing, while the time between dry spells is increasing), might have a significant impact on terrestrial ecosystems. Since productivity is already constrained by the availability of water, these changes are expected to have an impact on the dynamics of the community, population, and growth of plant in arid conditions [96].

As a result, it is anticipated that these species' benefits for human well-being will diminish in the future, and the services of ecosystems may be adversely impacted [3,79].

The species' geographic spread can also be impacted by the process of seed dispersal, the presence of various plant and animal species, and human activities such as invasive species, fires, and ecotourism [3]. Additionally, the role of several animal and bird species, such as magpies, jays, ravens, and squirrels, which are available in the KRI, must be taken into account as biological variables in the species distribution [9,97].

Besides mean temperature, annual precipitation, and precipitation seasonally, particularly for *C. azarolus,* the model showed that slope, with a contribution of 7.2%, is another important element affecting the species' habitat dispersal. It has been reported by [98] that the slope and aspect determine how much solar energy the mountain forest receives over the duration of a day. Additionally, they have an impact on the microenvironment of forest plants, influencing factors including air temperature, soil moisture, and humidity [9,99,100]. Moreover, for *C. monogyna,* the mean diurnal temperature (Bio2), with the contribution of 19%, has an important impact on species distribution; this result was indicated in some research in the Central Zagros of Iran [101]. As a result, several species will go to high latitudes or high elevations as a result of greenhouse gas emissions, while others will stay in their location through physiological or phenological changes [72,92,102].

The prediction of our model showed that with the shift of *C. azarolus* and *C. monogyna,* the differences between the current altitude and greater altitude would steadily increase, although the direction of centroid movement of the two species would change at different periods, in which they are anticipated to migrate toward latitudinal positions where mixed forests are more prevalent, in the east and southeast. Such shifts could have an important impression on the survival and spread of species, and through the use of predictive modeling tools expecting range shifts could include the identification of vulnerable species' refuges, which will aid in long-term conservation [82,103,104]. Moreover, it was possible to forecast the current distribution of the two species in this overlapped region since the highly appropriate habitats of the two *Crataegus* species overlapped. As a result, two GCMs, around 7626.53 km^2 (14.80%) and 7351.45 km^2 (14.27%), respectively, as a total of the study area (51,520.80 km^2), were discovered in the overlapped region, demonstrating the high ecological habitat between the two species, as shown in Figures 11 and 12 and Tables 9 and 10). In general, plants that are closely related have similar mechanisms for adapting to their environments during the course of evolution, and it was therefore expected that the two species' overlapping ecological habitats and evolutionary relationships would be correlated [72,105].

Table 9. Overlap habitat areas for *C. azarolus* and *C. monogyna* under GCM BCC-CSM2-MR in the KRI.

Class	Area	%
Unsuitable for both species	37,750.15	73.27
Suitable for *C. azarolus* only	5449.10	10.58
Suitable for *C. monogyna* only	695.02	1.35
Suitable for both species	7626.53	14.80
Total area	51,520.80	100.00

Table 10. Overlap habitat areas for *C. azarolus* and *C. monogyna* under GCM CNRM-CM6-1 in KRI.

Class	Area	%
Unsuitable for both species	38,147.63	74.04
Suitable for *C. azarolus* only	5283.82	10.26
Suitable for *C. monogyna* only	737.90	1.43
Suitable for both species	7351.45	14.27
Total area	51,520.80	100.00

4.3. Implications for Conservation

The conservation of biological diversity and management of natural resources are very significant matters, and understanding how these elements interact and affect species' coexistence and production is essential to developing future strategies [106]. The mountain forests of the KRI experience a number of issues that can be attributed to natural, human, and ineffective policies, including wars and the economic blockade, and the intensity of human activities that exert pressure and cause landscape fragmentation, such as the opening of fields, the extraction of wood resources, and the recurrence of fires, which can be made worse in light of climate change. As a result, they are unable to function normally [14]. Moreover, these dangers will continue to rise as the climate changes [9].

Determining the primary forces influencing the species' distribution in this region might yield useful knowledge for conservation and management efforts, as well as for the related biodiversity of the woods in the KRI and Iraq. They also provide useful benchmarking information for further studies on the forest ecosystem. Although these mountain forests are the natural habitat for *C. azarolus* and *C. monogyna*, the species' future possible range will be toward the mountainous regions to the east and southeast of the KRI. Therefore, by creating national parks and protected areas and adopting forest management policies, the present emphasis on conservation priority should concentrate primarily on places where the species overlap. Model outputs (i.e., continuous probability maps) integrated with GIS geospatial techniques will produce more sensible maps for the purpose of conservation and management actions. Management actions require detailed categorized maps of the target species that will possibly convince policy makers to take actions. The range overlap (Figure 11; Table 9; Figure 12; Table 10), categorized suitability classes (e.g., Figures 4 and 5), and spatial representation of the species' distributional shift (migration) (e.g., Figures A1 and A2), created in this study within a GIS environment after the Maxent modeling, supports the need of integrating GIS geospatial techniques and Maxent modeling in order to establish sensible recommendations for conservation efforts.

In this study, we recommend that: (1) mountains with mixed deciduous forests are crucial environments for the species now and in the future, making them a top priority for conservation efforts; (2) human activities such as cutting and clearing of the forests must be controlled by immediately establishing a monitoring and management policy; (3) the presence of overlapping habitats indicates a high level of biodiversity, and protecting these places should be a current priority; and (4) to lessen disturbances, eco-friendly tourist corridors should be created.

There were some limitations we faced during this research: in some mountainous areas of the KRI, the Sulaimani governorate in particular, we were not allowed to collect samples due to the political circumstances of the area. Owing to the existence of land mines in some other areas, collecting samples in them was unsafe.

5. Conclusions

Evaluating the distributional effects of changes in climate for *C. azarolus* and *C. monogyna* is essential for the preservation of the species across the KRI's mountain habitat. The investigation results indicate the increasing temperature and decreasing precipitation in the wake of climate change in the region, and the overall suitable habitats for *Crataegus* would contract under the 126, 245, and 585 SSP climate change scenarios for both the BCC-CSM2-MR and CNRM–CM6–1 global climatic models. The direction of the habitat shift, as demonstrated by the modeling, would be southeastward for the three-time windows 2041–2060, 2061–2080, and 2081–2100 in the KRI. Nevertheless, in the KRI, the distribution of *C. azarolus* and *C. monogyna* was mostly controlled by temperature and precipitation. Under the two future climate models, the suitable habitat range for *C. azarolus* will reduce by 11,913.98 km^2 (14.35%) and 12,030.16 km^2 (16.18%). For *C. monogyna*, the suitable habitat range reduction would be by 8097.77 km^2 (13.94%) and 8117.25 km^2 (13.73%). It may cause the population to decline in the future, for *C. azarolus* would be more than *C. monogyna* because *C. azarolus* is distributed widely and is the dominant *Crataegus* species in the KRI.

In addition, continuous challenges created by humans, such as war and clearing land for development, as well as climate change, remain serious. Moreover, the lower elevation is unfavorable for this species due to environmental factors, such as temperature and rainfall, which affect *C. azarolus'* habitat. Additionally, the species' potential range extends mostly to the southeast and east mountains. The study can offer crucial *Crataegus* management information and a warning to managers to preserve biodiversity in places where some species risk extinction in the future. This study acts as a warning that it is effective for predicting the temporal and geographical patterns of range shifts for *Crataegus* species. Machine-learning modeling integrated with geospatial techniques is a useful means of assessing the spatial pattern of species' distributions over space and time.

Author Contributions: N.R.K. conceived and designed the study; K.O.R. performed field surveys, data collection, analysis, and writing; N.R.K. also participated in analysis, writing, and compiling the final version of the manuscript. All authors have read and agreed to the published version of the manuscript.

Funding: This research received no external funding.

Institutional Review Board Statement: Not applicable.

Informed Consent Statement: Not applicable.

Data Availability Statement: Available on reasonable request.

Acknowledgments: We appreciate the assistance of the Kurdistan Botanical Foundation in identifying the plant species. We greatly appreciate the cooperation and help from the University of Sulaimani, especially the Department of Biology. We want to express our gratitude to everyone who helped to achieve our fieldwork.

Conflicts of Interest: The authors declare no conflict of interest.

Appendix A

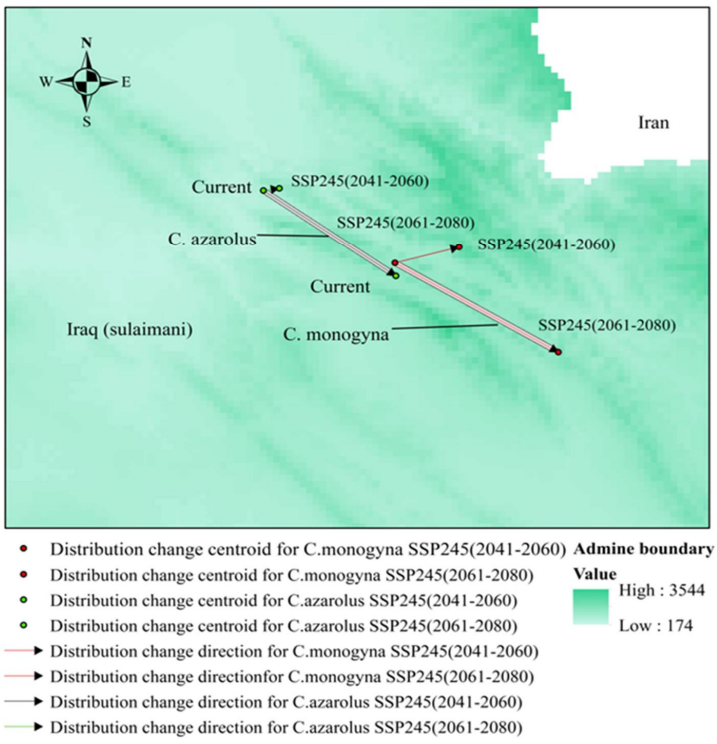


Figure A1. Density of the distribution change, its direction, and its magnitude (core) of *C. azarolus* and *C. monogyna*. The direction of the distribution change under the different scenarios in the GCM model (BCC-CSM2-MR) is shown by the head of the arrow, while the current centroid is represented by the tail.

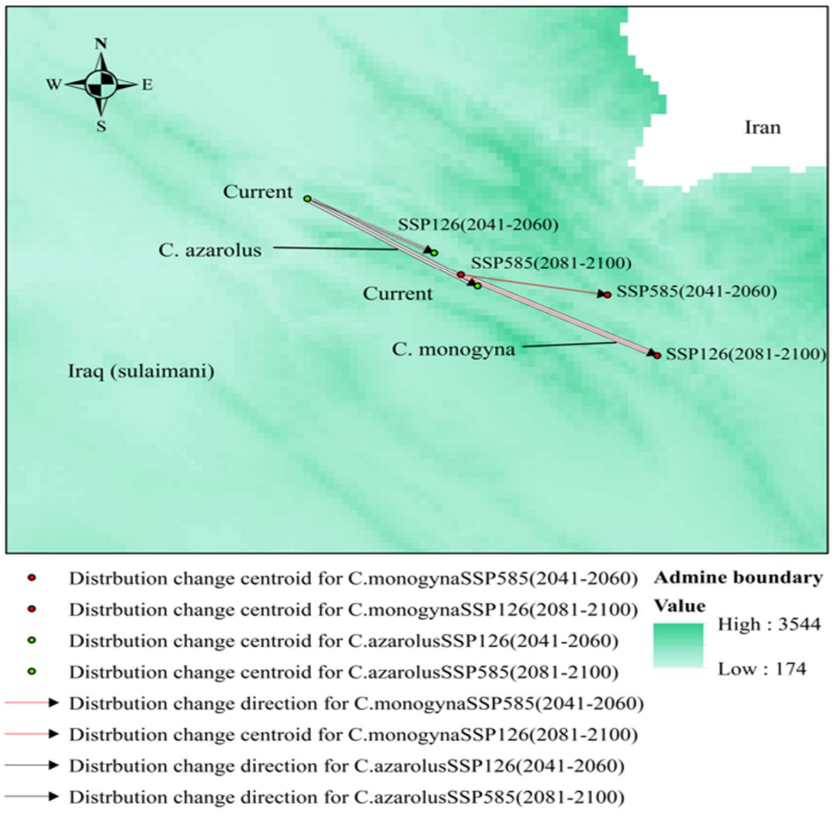


Figure A2. Density of the distribution change, its direction, and its magnitude (core) of *C. azarolus* and *C. monogyna*. The direction of the distribution change under the different scenarios in the GCM model (CNRM-CM6-1) is shown by the head of the arrow, while the current centroid is represented by the tail.

Table A1. Selecting environmental factors for modeling (the variables highlighted are used in building the model).

Variables	Code and Unit
Annual mean temperature	**Bio1 (°C)**
Mean diurnal range	**Bio2 (°C)**
Isothermality (Bio2/Bio7)	Bio3 (×100)
Temperature seasonality	Bio4 (standard deviation × 100)
Max temperature of warmest month	Bio5 (°C)
Min temperature of coldest month	Bio6 (°C)
Temperature annual range	Bio7 (Bio5-Bio6) (°C)
Mean temperature of wettest quarter	Bio8 (°C)
Mean temperature of driest quarter	Bio9 (°C)
Mean temperature of warmest quarter	Bio10 (°C)
Mean temperature of coldest quarter	Bio11 (°C)
Annual precipitation	**Bio12 (mm)**
Precipitation of wettest month	Bio13 (mm)
Precipitation of driest month	Bio14 (mm)
Precipitation seasonality (coefficient of variation)	**Bio15 (mm)**
Precipitation of wettest quarter	Bio16 (mm)
Precipitation of driest quarter	Bio17 (mm)
Precipitation of warmest quarter	Bio18 (mm)
Precipitation of coldest quarter	Bio19 (mm)
Slope	**Slope (degree)**
Aspect	**Aspect (degree)**
Soil pH	**Soil (parts hydrogen)**
Soil carbon	**gm·kg^{-1}**
Soil moisture	Soil moisture (mm)

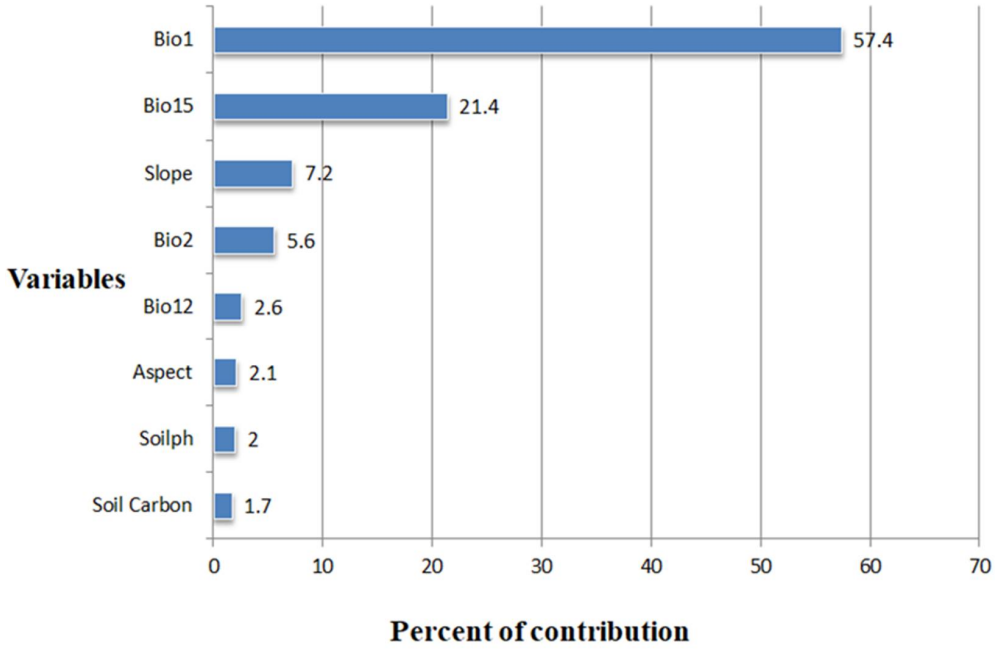


Figure A3. A selection of environmental factors and the percentage of each contributing to the Maxent model for *C. azarolus* in the KRI. (Bio1: annual mean temperature, Bio15: precipitation seasonality (coefficient of variation), Bio2: mean diurnal range, Bio12: annual precipitation).

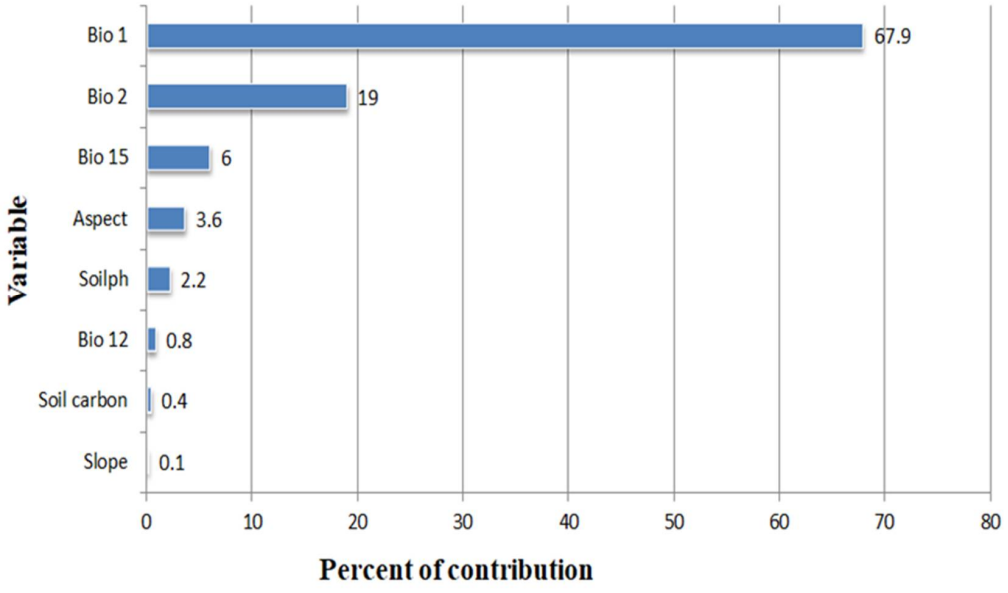


Figure A4. A selection of environmental factors and the percentage of each contributing to the Maxent model for *C. monogyna* in KRI. (Bio1: annual mean temperature, Bio15: precipitation seasonality (coefficient of variation), Bio2: mean diurnal range, Bio12: annual precipitation).

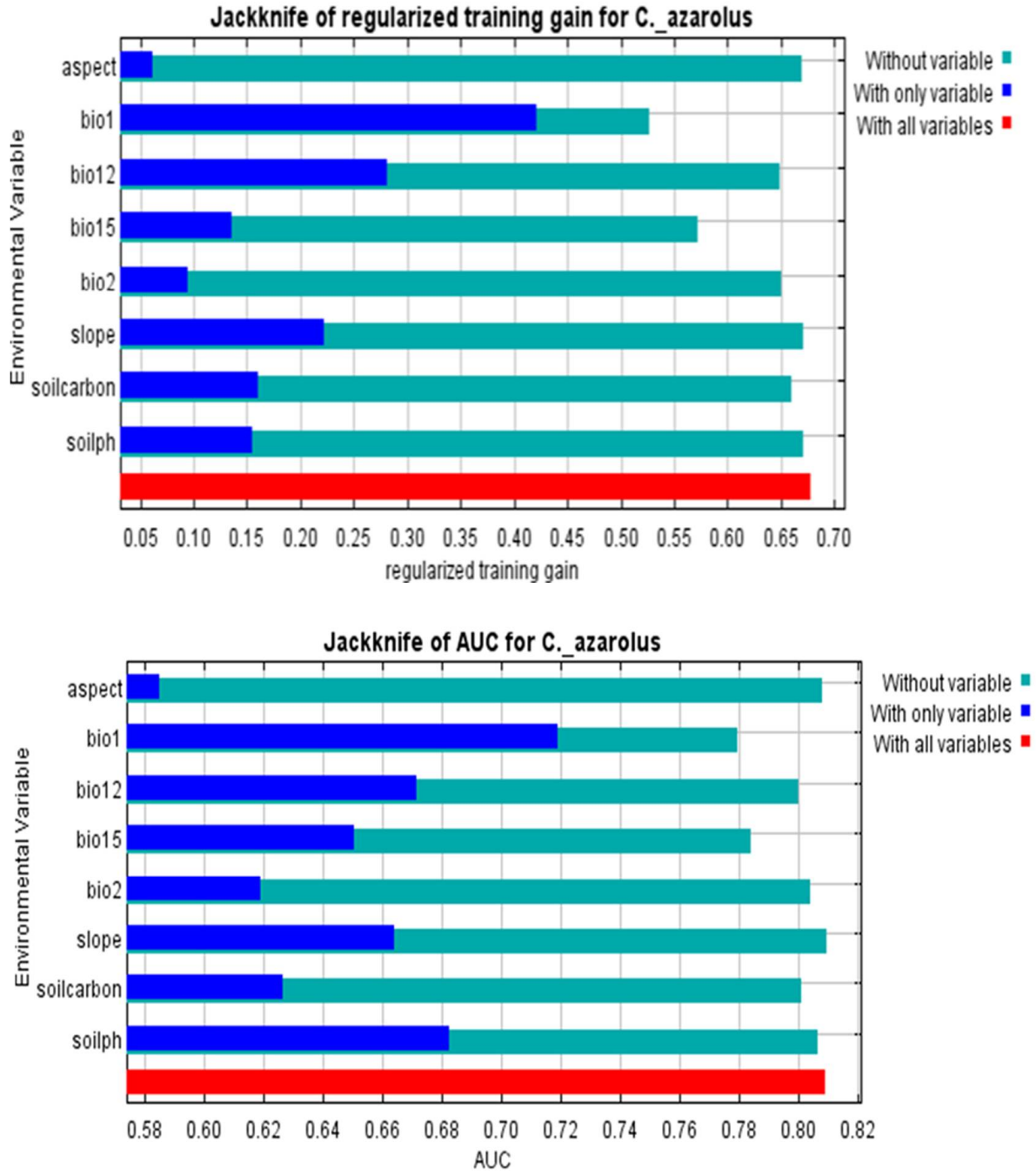


Figure A5. The relevance of environmental factors is assessed using the Jackknife test and training with regularized phase gains (%) and metric of AUC gain (%) for *C. azarolus*.

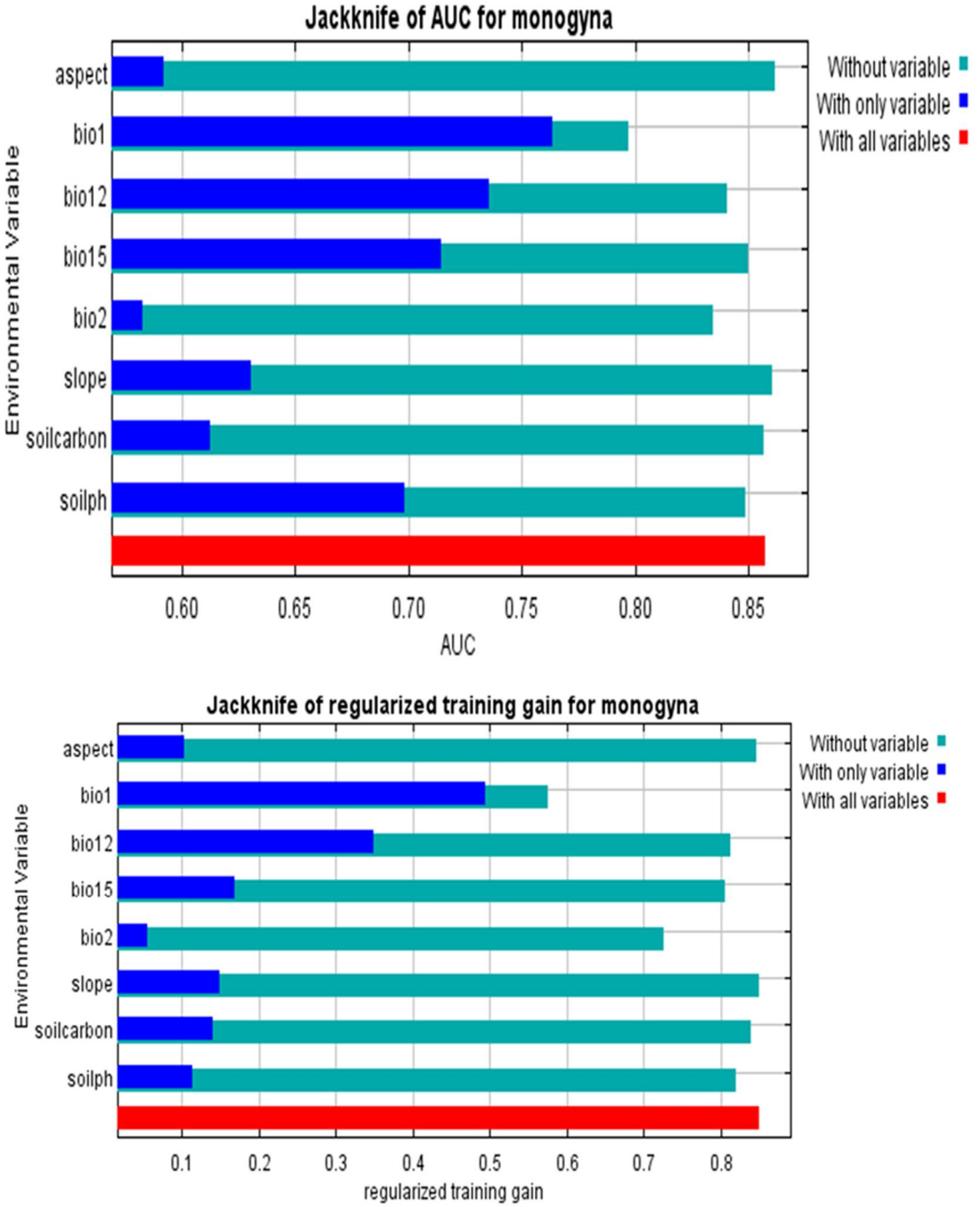


Figure A6. The relevance of environmental factors is assessed using the Jackknife test and training with regularized phase gains (%) and metric of AUC gain (%) for *C. monogyna*.

References

1. Christensen, K.I. Revision of Crataegus sect. Crataegus and Nothosect. Crataeguineae (Rosaceae-Maloideae) in the old world. *Syst. Bot. Monogr.* **1992**, *35*, 1–199. [CrossRef]
2. Özcan, M.; Hacıseferoğulları, H.; Marakoğlu, T.; Arslan, D. Hawthorn (*Crataegus* spp.) fruit: Some physical and chemical properties. *J. Food Eng.* **2005**, *69*, 409–413. [CrossRef]
3. Naghipour, A.A.; Asl, S.T.; Ashrafzadeh, M.R.; Haidarian, M. Predicting the Potential Distribution of *Crataegus azarolus* L. under Climate Change in Central Zagros, Iran. *J. Wildl. Biodivers.* **2021**, *5*, 28–43.

4. Zeravan, A.S.; Shahbaz, S.I.; AL Maa, A.M. Numerical Taxonomy for Genus *Crataegus* L. (*Rosaceae*) in North of Iraq. *Rafidain J. Sci.* **2007**, *18*, 1–15.
5. Gurlen, A.; Gundogdu, M.; Ozer, G.; Ercisli, S.; Duralija, B. Primary, secondary metabolites and molecular characterization of hawthorn (*Crataegus* spp.) genotypes. *Agronomy* **2020**, *10*, 1731. [CrossRef]
6. Shahbaz, S.E.; Sadeq, Z.A. Crataegus azarolus var. sharania (*Rosaceae*), a new variety for the flora of Iraq. *Nord. J. Bot.* **2003**, *23*, 713–717. [CrossRef]
7. Saadatian, M.; Peshawa, F.; Asiaban, K.; Karzan, A.; Muhammad, H. Determination of biochemical content and some pomological characteristics of 4 Hawthorn species (*Crataegus* spp.) grown in Erbil Province, Kregion, Iraq. *Adv. Environ. Biol.* **2014**, *8*, 2465–2469.
8. Al-Ansari, N. Topography and climate of Iraq. *J. Earth Sci. Geotech. Eng.* **2021**, *11*, 1–13. [CrossRef]
9. Khwarahm, N.R. Mapping current and potential future distributions of the oak tree (*Quercus aegilops*) in the Kurdistan Region, Iraq. *Ecol. Process.* **2020**, *9*, 56. [CrossRef]
10. Ahmadloo, F.; Kochaksaraei, M.T.; Azadi, P.; Hamidi, A.; Beiramizadeh, E. Effects of pectinase, BAP and dry storage on dormancy breaking and emergence rate of Crataegus pseudoheterophylla Pojark. *New For.* **2015**, *46*, 373–386. [CrossRef]
11. Nazhand, A.; Lucarini, M.; Durazzo, A.; Zaccardelli, M.; Cristarella, S.; Souto, S.B.; Silva, A.M.; Severino, P.; Souto, E.B.; Santini, A. Hawthorn (*Crataegus* spp.): An updated overview on its beneficial properties. *Forests* **2020**, *11*, 564. [CrossRef]
12. Özyurt, G.; Yücesan, Z.; Ak, N.; Oktan, E.; Üçler, A. Ecological and economic importance of studying propagation techniques of common hawthorn Crataegus monogyna Jacq. *Сибирский Лесной Журнал* **2019**, *4*, 63–67.
13. Khwarahm, N.R. Spatial modeling of land use and land cover change in Sulaimani, Iraq, using multitemporal satellite data. *Environ. Monit. Assess.* **2021**, *193*, 1–18. [CrossRef] [PubMed]
14. Nasser, M. Forests and forestry in Iraq: Prospects and limitations. *Commonw. For. Rev.* **1984**, *63*, 299–304.
15. Khwarahm, N.R. Modeling forest-shrubland fire susceptibility based on machine learning and geospatial approaches in mountains of Kurdistan Region, Iraq. *Arab. J. Geosci.* **2022**, *15*, 1–17. [CrossRef]
16. Adamo, N.; Al-Ansari, N.; Sissakian, V.; Fahmi, K.J.; Ali Abed, S. Climate Change: Droughts and Increasing Desertification in the Middle East, with Special Reference to Iraq. *Engineering* **2022**, *14*, 235–273. [CrossRef]
17. Alnasrawi, A. Iraq: Economic sanctions and consequences, 1990–2000. *Third World Q.* **2001**, *22*, 205–218. [CrossRef]
18. Monzón, J.; Moyer-Horner, L.; Palamar, M.B. Climate change and species range dynamics in protected areas. *Bioscience* **2011**, *61*, 752–761. [CrossRef]
19. Balaky, H.H.; Khalid, K.; Hasan, A.; Tahir, S.; Sedat, U.; Khedir, A. Estimation of total tannin and total phenolic content in plant (*Crataegus azarolus* L.) by orbital shaker technique. *Int. J. Agric. Environ. Food Sci.* **2021**, *5*, 1–6. [CrossRef]
20. Mahmud, S.A.; Al-Habib, O.A.; Bugoni, S.; Clericuzio, M.; Vidari, G. A new ursane-type triterpenoid and other constituents from the leaves of *Crataegus azarolus* var. *aronia*. *Nat. Prod. Commun.* **2016**, *11*, 1934578X1601101103. [CrossRef]
21. Beigmohamadi, M.; Rahmani, F.; Mirzaei, L. Study of Genetic Diversity Among Crataegus Species (Hawthorn) Using ISSR Markers in Northwestern of Iran. *Pharm. Biomed. Res.* **2021**, *7*, 59–66. [CrossRef]
22. Khadivi-Khub, A.; Karimi, S.; Kameli, M. Morphological diversity of naturally grown Crataegus monogyna (*Rosaceae*, *Maloideae*) in Central Iran. *Braz. J. Bot.* **2015**, *38*, 921–936. [CrossRef]
23. Moustafa, A.; Zaghloul, M.; Mansour, S.; Alotaibi, M. Conservation Strategy for protecting Crataegus x sinaica against climate change and anthropologic activities in South Sinai Mountains, Egypt. *Catrina Int. J. Environ. Sci.* **2019**, *18*, 1–6. [CrossRef]
24. Yanar, M.; Ercisli, S.; Yilmaz, K.; Sahiner, H.; Taskin, T.; Zengin, Y.; Akgul, I.; Celik, F. Morphological and chemical diversity among hawthorn (*Crataegus* spp.) genotypes from Turkey. *Sci. Res. Essays* **2011**, *6*, 35–38.
25. Hu, G.; Wang, Y.; Wang, Y.; Zheng, S.; Dong, W.; Dong, N. New insight into the phylogeny and taxonomy of cultivated and related species of Crataegus in China, based on complete chloroplast genome sequencing. *Horticulturae* **2021**, *7*, 301. [CrossRef]
26. Du, X.; Zhang, X.; Bu, H.; Zhang, T.; Lao, Y.; Dong, W. Molecular analysis of evolution and origins of cultivated hawthorn (*Crataegus* spp.) and related species in China. *Front. Plant Sci.* **2019**, *10*, 443. [CrossRef] [PubMed]
27. Hu, G.; Zheng, S.; Pan, Q.; Dong, N. The complete chloroplast genome of *Crataegus hupehensis* Sarg. (*Rosaceae*), a medicinal and edible plant in China. *Mitochondrial DNA Part B* **2021**, *6*, 315–317. [CrossRef]
28. Lyons, M.P.; Kozak, K.H. Vanishing islands in the sky? A comparison of correlation-and mechanism-based forecasts of range dynamics for montane salamanders under climate change. *Ecography* **2020**, *43*, 481–493. [CrossRef]
29. Di Pasquale, G.; Saracino, A.; Bosso, L.; Russo, D.; Moroni, A.; Bonanomi, G.; Allevato, E. Coastal pine-oak glacial refugia in the Mediterranean basin: A biogeographic approach based on charcoal analysis and spatial modelling. *Forests* **2020**, *11*, 673. [CrossRef]
30. Elith, J.; Leathwick, J.R. Species distribution models: Ecological explanation and prediction across space and time. *Annu. Rev. Ecol. Evol. Syst.* **2009**, *40*, 677–697. [CrossRef]
31. Franklin, J. *Mapping Species Distributions: Spatial Inference and Prediction*; Cambridge University Press: Cambridge, UK, 2010.
32. Elith, J.; Phillips, S.J.; Hastie, T.; Dudík, M.; Chee, Y.E.; Yates, C.J. A statistical explanation of MaxEnt for ecologists. *Divers. Distrib.* **2011**, *17*, 43–57. [CrossRef]
33. Phillips, S.J.; Anderson, R.P.; Schapire, R.E. Maximum entropy modeling of species geographic distributions. *Ecol. Model.* **2006**, *190*, 231–259. [CrossRef]

34. Støa, B.; Halvorsen, R.; Stokland, J.N.; Gusarov, V.I. How much is enough? Influence of number of presence observations on the performance of species distribution models. *Sommerfeltia* **2019**, *39*, 1–28. [CrossRef]
35. Phillips, S.J.; Dudík, M. Modeling of species distributions with Maxent: New extensions and a comprehensive evaluation. *Ecography* **2008**, *31*, 161–175. [CrossRef]
36. Sissakian, V.; Jabbar, M.A.; Al-Ansari, N.; Knutsson, S. Development of Gulley Ali Beg Gorge in Rawandooz Area, Northern Iraq. *Engineering* **2015**, *7*, 16–30. [CrossRef]
37. Khwarahm, N.R.; Ararat, K.; Qader, S.; Sabir, D.K. Modeling the distribution of the Near Eastern fire salamander (*Salamandra infraimmaculata*) and Kurdistan newt (*Neurergus derjugini*) under current and future climate conditions in Iraq. *Ecol. Inform.* **2021**, *63*, 101309. [CrossRef]
38. Townsend, C.; Guest, E. *1985 Flora of Iraq*; Ministry of Agriculture and Agrarian Reform: Baghdad, Iraq, 1966; Volume 2–8.
39. Morales, N.S.; Fernández, I.C.; Baca-González, V. MaxEnt's parameter configuration and small samples: Are we paying attention to recommendations? A systematic review. *PeerJ* **2017**, *5*, e3093. [CrossRef]
40. Bhatta, K.P.; Chaudhary, R.P.; Vetaas, O.R. A comparison of systematic versus stratified-random sampling design for gradient analyses: A case study in subalpine Himalaya, Nepal. *Phytocoenologia* **2012**, *42*, 191–202. [CrossRef]
41. Boakes, E.H.; McGowan, P.J.; Fuller, R.A.; Chang-qing, D.; Clark, N.E.; O'Connor, K.; Mace, G.M. Distorted views of biodiversity: Spatial and temporal bias in species occurrence data. *PLoS Biol.* **2010**, *8*, e1000385. [CrossRef]
42. Moreno, J.S.; Sandoval-Arango, S.; Palacio, R.D.; Alzate, N.F.; Rincón, M.; Gil, K.; Morales, N.G.; Harding, P.; Hazzi, N.A. Distribution Models and Spatial Analyses Provide Robust Assessments of Conservation Status of Orchid Species in Colombia: The Case of Lephantes mucronata. *Harv. Pap. Bot.* **2020**, *25*, 111–121. [CrossRef]
43. Boria, R.A.; Olson, L.E.; Goodman, S.M.; Anderson, R.P. Spatial filtering to reduce sampling bias can improve the performance of ecological niche models. *Ecol. Model.* **2014**, *275*, 73–77. [CrossRef]
44. Brown, J.L. SDM toolbox: A python-based GIS toolkit for landscape genetic, biogeographic and species distribution model analyses. *Methods Ecol. Evol.* **2014**, *5*, 694–700. [CrossRef]
45. Jafari, A.; Alipour, M.; Abbasi, M.; Soltani, A. *Distribution Modeling of Hawthorn (Crataegus azarolus L.) in Chaharmahal & Bakhtiari Province Using the Maximum Entropy Method*; SID: Singapore, 2019.
46. Elith, J.; Kearney, M.; Phillips, S. The art of modelling range-shifting species. *Methods Ecol. Evol.* **2010**, *1*, 330–342. [CrossRef]
47. Li, J.; Fan, G.; He, Y. Predicting the current and future distribution of three Coptis herbs in China under climate change conditions, using the MaxEnt model and chemical analysis. *Sci. Total Environ.* **2020**, *698*, 134141. [CrossRef] [PubMed]
48. Zhang, J.; Song, M.; Li, Z.; Peng, X.; Su, S.; Li, B.; Xu, X.; Wang, W. Effects of climate change on the distribution of Akebia quinata. *Predict. Manag. Clim.-Driven Range Shifts Plants* **2022**, *9*, 752682. [CrossRef]
49. Díaz, J.V.R.; González, F.d.B.J.-A.; Álvarez, P.Á.; García, M.Á.Á. Environmental niche and distribution of six deciduous tree species in the Spanish Atlantic region. *Iforest-Biogeosciences For.* **2014**, *8*, 214–221. [CrossRef]
50. Pecchi, M.; Marchi, M.; Burton, V.; Giannetti, F.; Moriondo, M.; Bernetti, I.; Bindi, M.; Chirici, G. Species distribution modelling to support forest management. A literature review. *Ecol. Model.* **2019**, *411*, 108817. [CrossRef]
51. Voldoire, A.; Saint-Martin, D.; Sénési, S.; Decharme, B.; Alias, A.; Chevallier, M.; Colin, J.; Guérémy, J.F.; Michou, M.; Moine, M.P. Evaluation of CMIP6 deck experiments with CNRM-CM6-1. *J. Adv. Modeling Earth Syst.* **2019**, *11*, 2177–2213. [CrossRef]
52. Brzozowski, M.; Pełechaty, M.; Bogawski, P. A winner or a loser in climate change? Modelling the past, current, and future potential distributions of a rare charophyte species. *Glob. Ecol. Conserv.* **2022**, *34*, e02038. [CrossRef]
53. Wu, T.; Lu, Y.; Fang, Y.; Xin, X.; Li, L.; Li, W.; Jie, W.; Zhang, J.; Liu, Y.; Zhang, L. The Beijing Climate Center climate system model (BCC-CSM): The main progress from CMIP5 to CMIP6. *Geosci. Model Dev.* **2019**, *12*, 1573–1600. [CrossRef]
54. Iqbal, Z.; Shahid, S.; Ahmed, K.; Ismail, T.; Khan, N.; Virk, Z.T.; Johar, W. Evaluation of global climate models for precipitation projection in sub-Himalaya region of Pakistan. *Atmos. Res.* **2020**, *245*, 105061. [CrossRef]
55. Mahmoodi, S.; Heydari, M.; Ahmadi, K.; Khwarahm, N.R.; Karami, O.; Almasieh, K.; Naderi, B.; Bernard, P.; Mosavi, A. The current and future potential geographical distribution of Nepeta crispa Willd., an endemic, rare and threatened aromatic plant of Iran: Implications for ecological conservation and restoration. *Ecol. Indic.* **2022**, *137*, 108752. [CrossRef]
56. Katiraie-Boroujerdy, P.S.; Asanjan, A.A.; Chavoshian, A.; Hsu, K.l.; Sorooshian, S. Assessment of seven CMIP5 model precipitation extremes over Iran based on a satellite-based climate data set. *Int. J. Climatol.* **2019**, *39*, 3505–3522. [CrossRef]
57. Zuur, A.F.; Ieno, E.N.; Elphick, C.S. A protocol for data exploration to avoid common statistical problems. *Methods Ecol. Evol.* **2010**, *1*, 3–14. [CrossRef]
58. Brown, J.L.; Bennett, J.R.; French, C.M. SDMtoolbox 2.0: The next generation Python-based GIS toolkit for landscape genetic, biogeographic and species distribution model analyses. *PeerJ* **2017**, *5*, e4095. [CrossRef] [PubMed]
59. Dormann, C.F.; Elith, J.; Bacher, S.; Buchmann, C.; Carl, G.; Carré, G.; Marquéz, J.R.G.; Gruber, B.; Lafourcade, B.; Leitão, P.J. Collinearity: A review of methods to deal with it and a simulation study evaluating their performance. *Ecography* **2013**, *36*, 27–46. [CrossRef]
60. Li, J.; Chang, H.; Liu, T.; Zhang, C. The potential geographical distribution of Haloxylon across Central Asia under climate change in the 21st century. *Agric. For. Meteorol.* **2019**, *275*, 243–254. [CrossRef]
61. Qin, A.; Liu, B.; Guo, Q.; Bussmann, R.W.; Ma, F.; Jian, Z.; Xu, G.; Pei, S. Maxent modeling for predicting impacts of climate change on the potential distribution of Thuja sutchuenensis Franch., an extremely endangered conifer from southwestern China. *Glob. Ecol. Conserv.* **2017**, *10*, 139–146. [CrossRef]

62. Elith, J.; Graham, C.H.; Anderson, R.P.; Dudík, M.; Ferrier, S.; Guisan, A.; Hijmans, R.J.; Huettmann, F.; Leathwick, J.R.; Lehmann, A. Novel methods improve prediction of species' distributions from occurrence data. *Ecography* **2006**, *29*, 129–151. [CrossRef]
63. Phillips, S.J.; Dudík, M.; Schapire, R.E. A maximum entropy approach to species distribution modeling. In Proceedings of the Twenty-First International Conference on Machine Learning, New York, NY, USA, 4–8 June 2004; p. 83.
64. Merow, C.; Smith, M.J.; Silander, J.A., Jr. A practical guide to MaxEnt for modeling species' distributions: What it does, and why inputs and settings matter. *Ecography* **2013**, *36*, 1058–1069. [CrossRef]
65. Phillips, S.J.; Anderson, R.P.; Dudík, M.; Schapire, R.E.; Blair, M.E. Opening the black box: An open-source release of Maxent. *Ecography* **2017**, *40*, 887–893. [CrossRef]
66. Zhang, S.; Liu, X.; Li, R.; Wang, X.; Cheng, J.; Yang, Q.; Kong, H. AHP-GIS and MaxEnt for delineation of potential distribution of Arabica coffee plantation under future climate in Yunnan, China. *Ecol. Indic.* **2021**, *132*, 108339. [CrossRef]
67. Fielding, A.H.; Bell, J.F. A review of methods for the assessment of prediction errors in conservation presence/absence models. *Environ. Conserv.* **1997**, *24*, 38–49. [CrossRef]
68. Abolmaali, S.M.-R.; Tarkesh, M.; Bashari, H. MaxEnt modeling for predicting suitable habitats and identifying the effects of climate change on a threatened species, Daphne mucronata, in central Iran. *Ecol. Inform.* **2018**, *43*, 116–123. [CrossRef]
69. Yang, X.-Q.; Kushwaha, S.; Saran, S.; Xu, J.; Roy, P. Maxent modeling for predicting the potential distribution of medicinal plant, Justicia adhatoda L. in Lesser Himalayan foothills. *Ecol. Eng.* **2013**, *51*, 83–87. [CrossRef]
70. Pearce, J.; Ferrier, S. Evaluating the predictive performance of habitat models developed using logistic regression. *Ecol. Model.* **2000**, *133*, 225–245. [CrossRef]
71. Leroy, B.; Delsol, R.; Hugueny, B.; Meynard, C.N.; Barhoumi, C.; Barbet-Massin, M.; Bellard, C. Without quality presence–absence data, discrimination metrics such as TSS can be misleading measures of model performance. *J. Biogeogr.* **2018**, *45*, 1994–2002. [CrossRef]
72. Jiang, R.; Zou, M.; Qin, Y.; Tan, G.; Huang, S.; Quan, H.; Zhou, J.; Liao, H. Modeling of the potential geographical distribution of three Fritillaria species under climate change. *Front. Plant Sci.* **2021**, *12*, 749838. [CrossRef]
73. Yan, X.; Wang, S.; Duan, Y.; Han, J.; Huang, D.; Zhou, J. Current and future distribution of the deciduous shrub Hydrangea macrophylla in China estimated by MaxEnt. *Ecol. Evol.* **2021**, *11*, 16099–16112. [CrossRef]
74. Ouyang, X.; Chen, A.; Lin, H. Predicting the potential distribution of pine wilt disease in China under climate change. *Authorea Prepr.* **2022**. [CrossRef]
75. Saha, A.; Rahman, S.; Alam, S. Modeling current and future potential distributions of desert locust Schistocerca gregaria (Forskål) under climate change scenarios using MaxEnt. *J. Asia-Pac. Biodivers.* **2021**, *14*, 399–409. [CrossRef]
76. Mulieri, P.R.; Patitucci, L.D. Using ecological niche models to describe the geographical distribution of the myiasis-causing Cochliomyia hominivorax (Diptera: Calliphoridae) in southern South America. *Parasitol. Res.* **2019**, *118*, 1077–1086. [CrossRef] [PubMed]
77. Al-Qaddi, N.; Vessella, F.; Stephan, J.; Al-Eisawi, D.; Schirone, B. Current and future suitability areas of kermes oak (*Quercus coccifera* L.) in the Levant under climate change. *Reg. Environ. Change* **2017**, *17*, 143–156. [CrossRef]
78. Çoban, H.O.; Örücü, Ö.K.; Arslan, E.S. MaxEnt modeling for predicting the current and future potential geographical distribution of Quercus libani Olivier. *Sustainability* **2020**, *12*, 2671. [CrossRef]
79. Arslan, E.S.; Akyol, A.; Örücü, Ö.K.; Sarıkaya, A.G. Distribution of rose hip (*Rosa canina* L.) under current and future climate conditions. *Reg. Environ. Change* **2020**, *20*, 1–13. [CrossRef]
80. Körner, C.; Basler, D.; Hoch, G.; Kollas, C.; Lenz, A.; Randin, C.F.; Vitasse, Y.; Zimmermann, N.E. Where, why and how? Explaining the low-temperature range limits of temperate tree species. *J. Ecol.* **2016**, *104*, 1076–1088. [CrossRef]
81. Zohary, M. *Geobotanical Foundations of the Middle East*; Fischer: Brownsville, TX, USA, 1973.
82. Rajpoot, R.; Adhikari, D.; Verma, S.; Saikia, P.; Kumar, A.; Grant, K.R.; Dayanandan, A.; Kumar, A.; Khare, P.K.; Khan, M.L. Climate models predict a divergent future for the medicinal tree Boswellia serrata Roxb. in India. *Glob. Ecol. Conserv.* **2020**, *23*, e01040. [CrossRef]
83. Zhang, L.; Zhu, L.; Li, Y.; Zhu, W.; Chen, Y. Maxent modelling predicts a shift in suitable habitats of a subtropical evergreen tree (*Cyclobalanopsis glauca* (*Thunberg*) *Oersted*) under climate change scenarios in China. *Forests* **2022**, *13*, 126. [CrossRef]
84. Junttila, O.; Nilsen, J. Growth and development of northern forest trees as affected by temperature and light. *For. Dev. Cold Clim.* **1993**, 43–57.
85. Zhao, M.; Running, S.W. Drought-induced reduction in global terrestrial net primary production from 2000 through 2009. *Science* **2010**, *329*, 940–943. [CrossRef]
86. Wu, C.; Chen, J. The use of precipitation intensity in estimating gross primary production in four northern grasslands. *J. Arid. Environ.* **2012**, *82*, 11–18. [CrossRef]
87. Sepúlveda, M.; Bown, H.E.; Miranda, M.D.; Fernández, B. Impact of rainfall frequency and intensity on inter-and intra-annual satellite-derived EVI vegetation productivity of an Acacia caven shrubland community in Central Chile. *Plant Ecol.* **2018**, *219*, 1209–1223. [CrossRef]
88. Bertrand, R.; Lenoir, J.; Piedallu, C.; Riofrío-Dillon, G.; De Ruffray, P.; Vidal, C.; Pierrat, J.-C.; Gégout, J.-C. Changes in plant community composition lag behind climate warming in lowland forests. *Nature* **2011**, *479*, 517–520. [CrossRef] [PubMed]

89. Braunisch, V.; Coppes, J.; Arlettaz, R.; Suchant, R.; Zellweger, F.; Bollmann, K. Temperate mountain forest biodiversity under climate change: Compensating negative effects by increasing structural complexity. *PLoS ONE* **2014**, *9*, e97718. [CrossRef] [PubMed]
90. Khwarahm, N.R.; Ararat, K.; HamadAmin, B.A.; Najmaddin, P.M.; Rasul, A.; Qader, S. Spatial distribution modeling of the wild boar (*Sus scrofa*) under current and future climate conditions in Iraq. *Biologia* **2022**, *77*, 369–383. [CrossRef]
91. Hansen, W.D.; Braziunas, K.H.; Rammer, W.; Seidl, R.; Turner, M.G. It takes a few to tango: Changing climate and fire regimes can cause regeneration failure of two subalpine conifers. *Ecology* **2018**, *99*, 966–977. [CrossRef]
92. Zhang, K.; Yao, L.; Meng, J.; Tao, J. Maxent modeling for predicting the potential geographical distribution of two peony species under climate change. *Sci. Total Environ.* **2018**, *634*, 1326–1334. [CrossRef]
93. Zhao, L.; Wang, L.; Xiao, H.; Liu, X.; Cheng, G.; Ruan, Y. The effects of short-term rainfall variability on leaf isotopic traits of desert plants in sand-binding ecosystems. *Ecol. Eng.* **2013**, *60*, 116–125. [CrossRef]
94. Yan, H.; Liang, C.; Li, Z.; Liu, Z.; Miao, B.; He, C.; Sheng, L. Impact of precipitation patterns on biomass and species richness of annuals in a dry steppe. *PLoS ONE* **2015**, *10*, e0125300.
95. Tielbörger, K.; Salguero-Gómez, R. Some like it hot: Are desert plants indifferent to climate change? In *Progress in Botany*; Springer: Berlin/Heidelberg, Germany, 2014; pp. 377–400.
96. Miranda, J.d.D.; Padilla, F.; Lázaro, R.; Pugnaire, F. Do changes in rainfall patterns affect semiarid annual plant communities? *J. Veg. Sci.* **2009**, *20*, 269–276. [CrossRef]
97. Salim, M.; Ararat, K.; Abdulrahman, O.F. A provisional checklist of the Birds of Iraq. *Iraq Marsh Bull.* **2010**, *5*, 56–95.
98. Desta, F.; Colbert, J.; Rentch, J.S.; Gottschalk, K.W. Aspect induced differences in vegetation, soil, and microclimatic characteristics of an Appalachian watershed. *Castanea* **2004**, *69*, 92–108. [CrossRef]
99. Fekedulegn, D.; Hicks, R.R., Jr.; Colbert, J. Influence of topographic aspect, precipitation and drought on radial growth of four major tree species in an Appalachian watershed. *For. Ecol. Manag.* **2003**, *177*, 409–425. [CrossRef]
100. Rosenberg, N.J.; Blad, B.L.; Verma, S.B. *Microclimate: The Biological Environment*; John Wiley & Sons: Hoboken, NJ, USA, 1983.
101. Sangoony, H.; Vahabi, M.; Tarkesh, M.; Soltani, S. Range shift of Bromus tomentellus Boiss. as a reaction to climate change in Central Zagros, Iran. *Appl. Ecol. Environ. Res.* **2016**, *14*, 85–100. [CrossRef]
102. Faticov, M.; Abdelfattah, A.; Roslin, T.; Vacher, C.; Hambäck, P.; Blanchet, F.G.; Lindahl, B.D.; Tack, A.J. Climate warming dominates over plant genotype in shaping the seasonal trajectory of foliar fungal communities on oak. *New Phytol.* **2021**, *231*, 1770–1783. [CrossRef]
103. Monteith, K.L.; Klaver, R.W.; Hersey, K.R.; Holland, A.A.; Thomas, T.P.; Kauffman, M.J. Effects of climate and plant phenology on recruitment of moose at the southern extent of their range. *Oecologia* **2015**, *178*, 1137–1148. [CrossRef]
104. Beaumont, L.J.; Esperón-Rodríguez, M.; Nipperess, D.A.; Wauchope-Drumm, M.; Baumgartner, J.B. Incorporating future climate uncertainty into the identification of climate change refugia for threatened species. *Biol. Conserv.* **2019**, *237*, 230–237. [CrossRef]
105. Milanesi, P.; Caniglia, R.; Fabbri, E.; Puopolo, F.; Galaverni, M.; Holderegger, R. Combining Bayesian genetic clustering and ecological niche modeling: Insights into wolf intraspecific genetic structure. *Ecol. Evol.* **2018**, *8*, 11224–11234. [CrossRef]
106. Eulewi, H.K.; Hasan, A. Monitoring of the temporal changes in the forests of northern Iraq through the directed classification and the index of natural vegetative difference. *Plant Arch.* **2020**, *20*, 5745–5750.